UNIVERSIDADE ESTADUAL PAULISTA
"JÚLIO DE MESQUITA FILHO"
Campus de Ilha Solteira

PROGRAMA DE PÓS-GRADUAÇÃO EM ENGENHARIA MECÂNICA

Jose Camilo Carranza López

Comparison between the Performances of a Linear Isolator and an Isolator with a Geometrically Nonlinear Damper

Ilha Solteira
2013

UNIVERSIDADE ESTADUAL PAULISTA
"JÚLIO DE MESQUITA FILHO"
Campus de Ilha Solteira

PROGRAMA DE PÓS-GRADUAÇÃO EM ENGENHARIA MECÂNICA

Jose Camilo Carranza López

Comparison between the Performances of a Linear Isolator and an Isolator with a Geometrically Nonlinear Damper

Dissertação apresentada à Faculdade de Engenharia – UNESP – Campus de Ilha Solteira, para obtenção do título de Mestre em Engenharia Mecânica.
Área de Conhecimento: Mecânica dos Sólidos

Prof. Dr. Michael John Brennan
Orientador

Ilha Solteira
2013

FICHA CATALOGRÁFICA
Desenvolvido pelo Serviço Técnico de Biblioteca e Documentação

C864c

Carranza López, José Camilo.
Comparison between the performances of a linear isolator and an isolator with a geometrically nonlinear damper: comparison between the performances of a linear isolator and an isolator with a geometrically nonlinear damper / José Camilo Carranza López. -- Ilha Solteira: [s.n.], 2013
75 f. : il.

Dissertação (mestrado) - Universidade Estadual Paulista. Faculdade de Engenharia de Ilha Solteira. Área de conhecimento: Mecânica dos sólidos, 2013

Orientador: Michael John Brennan
Inclui bibliografia

1. Isolamento de vibrações. 2. Amortecimento não linear. 3. Serie de Fourier.

unesp UNIVERSIDADE ESTADUAL PAULISTA
CAMPUS DE ILHA SOLTEIRA
FACULDADE DE ENGENHARIA DE ILHA SOLTEIRA

CERTIFICADO DE APROVAÇÃO

TÍTULO: Comparison between the Performances of a Linear Isolator and an Isolator with a Geometrically Nonlinear Damper

AUTOR: JOSE CAMILO CARRANZA LOPEZ

ORIENTADOR: Prof. Dr. MICHAEL JOHN BRENNAN

Aprovado como parte das exigências para obtenção do Título de Mestre em Engenharia Mecânica , Área: MECANICA DOS SÓLIDOS, pela Comissão Examinadora:

Prof. Dr. MICHAEL JOHN BRENNAN
Departamento de Engenharia Mecânica / Faculdade de Engenharia de Ilha Solteira

Prof. Dr. GILBERTO PECHOTO DE MELO
Departamento de Engenharia Mecânica / Faculdade de Engenharia de Ilha Solteira

Prof. Dr. PAULO JOSE PAUPITZ GONCALVES
Departamento de Engenharia Mecânica / Faculdade de Engenharia de Bauru

Data da realização: 21 de outubro de 2013.

To Paola …

who has always made me feel her unconditional love wherever I am, whatever I do; and who has always believed in my dreams no matter the circumstances.

ACKNOWLEDGMENT

I would like to thank my supervisor, Professor Mike Brennan for his great guidance and his wise advices, as well as for its patience and kindness. I really feel fortunate to have had such a wonderful person as supervisor, which has contributed largely to my academic and my personal life.

I would like to thank Professor Bin Tang for his valuable help and enriching conversations.

Thanks to my colleagues from Unesp, and my friends from Ilha Solteira: Natallie, Gabriella, Murilo, Giulio and Carlos for having made my time here nice and happy, and for having made me part of their beautiful group.

Special thanks to Paola and to my family for their infinite love and support; and to my Brazilian family (Flatmates): Marcos, Julio, Lucas, Flavio, Danilo and Paulo who has received me in Ilha and helped me during these years.

I would like to thank Capes (Coordenação de Aperfeiçoamento de Pessoal de Nível Superior) for the financial support.

“One’s destination is never a place, but a new way of seeing things”

Henry Miller

RESUMO

Nesta dissertação investiga-se o comportamento de um sistema de isolamento de vibrações de um grau de liberdade com amortecimento não linear. As transmissibilidades das forças e de movimento deste sistema são comparadas com as de um sistema de isolamento de vibrações linear. O sistema não linear é composto por uma mola e um amortecedor viscoso, ambos lineares, que estão acoplados a uma massa de modo tal que o amortecedor é perpendicular à mola. O sistema é excitado harmonicamente por um deslocamento da base ou por uma força na direção da mola. Quando o sistema é excitado por uma forca harmônica, as forças transmitidas através da mola e do amortecedor são analisadas separadamente, decompondo-as em termos dos seus harmônicos; permitindo assim determinar a contribuição individual de cada elemento no comportamento não linear do sistema como um todo. A transmissibilidade do sistema de isolamento não linear é calculada por meio de expressões analíticas validas para excitações com pequenas amplitudes, já para excitações com amplitudes grandes, calcula-se por meio de simulações numéricas.

Palavras-chave: Transmissibilidade de força. Transmissibilidade do deslocamento. Isolamento de vibrações não linear. Serie de Fourier.

ABSTRACT

In this work the behaviour of a single degree of freedom (SDOF) passive vibration isolation system with a geometrically nonlinear damper is investigated, and its displacement and force transmissibilities are compared with that of a linear system. The nonlinear system is composed of a linear spring and a linear viscous damper which are connected to a mass so that the damper is perpendicular to the spring. The system is excited with either a harmonic force or an imposed displacement of the base in the direction of the spring. When excited with a harmonic force, the forces transmitted through the spring and the damper are analysed separately by decomposing the forces in terms of their harmonics. This enables the effects of these elements to be studied and to determine how they contribute individually to the nonlinear behaviour of the system as a whole. The transmissibilities of the nonlinear isolation system are calculated using analytical expressions for small amplitudes of excitation and by using numerical simulations for high amplitudes of excitation.

Key words: Force transmissibility. Displacement transmissibility. Nonlinear vibration isolation. Fourier series.

LIST OF SYMBOLS

Symbol	Name	Units
m	Mass	[kilogram] – [kg]
a	Damper length	[meter] – [m]
t	Time	[seconds] – [s]
k	Stiffness	[kg/m]
c	Damping coefficient	[kg·s/m]
c_h	Horizontal damping coefficient	[kg·s/m]
c_{eq}	Equivalent damping coefficient	[kg·s/m]
h	Damper length in any position	[m]
x	Displacement of the mass	[m]
y	Displacement of the base	[m]
z	Relative displacement	[m]
$\dot{x}$	Velocity of the mass	[m/s]
$\dot{y}$	Velocity of the base	[m/s]
$\dot{z}$	Relative velocity	[m/s]
$\ddot{x}$	Acceleration of the mass	[m/s²]
$\ddot{y}$	Acceleration of the base	[m/ s²]
$\ddot{z}$	Relative acceleration	[m/ s²]
f_t	Transmitted force	[Newton] – [N]
f_h	Horizontal lineal damping force	[N]
f_e	Excitation force	[N]
f_k	Spring force	[N]
f_d	Damping force	[N]
X	Amplitude of the displacement of the mass	[m]
Y	Amplitude of the displacement of the base	[m]
E	Energy dissipated by the damping force	[Joule] – [J]
E_l	Energy dissipated by a linear damper	[J]
T	Non-dimensional Period	[--]
$\hat{y}$	Non-dimensional displacement of the base	[--]
$\hat{z}$	Non-dimensional relative displacement	[--]
$\hat{x}'$	Non-dimensional velocity of the mass	[--]
$\hat{y}'$	Non-dimensional velocity of the base	[--]
$\hat{z}'$	Non-dimensional relative velocity	[--]
$\hat{x}''$	Non-dimensional acceleration of the mass	[--]
$\hat{y}''$	Non-dimensional acceleration of the base	[--]
$\hat{z}''$	Non-dimensional relative acceleration	[--]
$\hat{X}$	Non-dimensional amplitude of the displacement of the mass	[--]
$\hat{Y}$	Non-dimensional amplitude of the displacement of the base	[--]
T_D	Displacement transmissibility	[--]

Symbol	Name	Units
ζ	Linear damping ratio	[--]
τ	Non-dimensional time	[--]
θ	Angle between the damper and the horizontal line	[radians] – [rad]
Ω_d	Frequency at which the force through the damper starts to dominate the transmissibility	[--]
ζ_{eq}	Equivalent damping ratio	[--]
ω	Excitation frequency	[rad/s]
ω_n	Natural frequency	[m]

CONTENT

1 INTRODUCTION

1.1 Background

Vibration is in many cases useful and desirable, e.g. in music or in medical treatments, but in most of the cases vibration is undesirable because of its detrimental effects on structures and on the human body. Excessive levels of noise from factories and vehicles engines as well as vibration transmitted through structures can cause discomfort in humans, and high amplitude vibrations can cause fatigue and damage in machinery and in structures. Nowadays there is a pressing demand for the protection of structural installations, nuclear reactors, mechanical components, and sensitive instruments from earthquake ground motion, shocks, and impact loads (IBRAHIM, 2008).

These detrimental effects have motivated diverse approaches to vibration control which can be divided mainly into three areas. The first is the reduction of the vibrational excitation at source, which is often impractical because of economic and practical reasons. The second is the modification of the physical properties of the receiver, which is the part of the system which receives the transmitted vibration. The third is called *vibration isolation*. In this approach the vibration is reduced by employing isolators between the vibration source and the receiver (YAN, 2007).

Vibration isolation is possibly the most widely used approach for vibration protection (RIVIN, 2003). It can be achieved by means of active, semi active and passive isolators placed between the source and the receiver. Active isolators usually perform well, reducing vibration to desirable levels over a wide range of excitation frequencies. However, computers and actuators are employed to modify the system response and they require a continuous supply of energy and have high costs. Semi-active isolators modify the properties of the system. They use small quantities of energy and have good performance at high excitation frequencies, but usually they have a complicated engineering design. A passive vibration isolator is composed of a spring and a damper located in parallel between the source and the receiver.

Passive vibration isolation systems can be linear or nonlinear depending on the form of the forces in the system. This dissertation concerns nonlinear passive vibration isolation. The main goal is to compare the performance of a nonlinear isolator with a geometrically nonlinear damper with of that a linear isolation system and to analyse the time histories of the transmitted forces.

1.2 Literature Review

In the past few years the interest in studying nonlinear isolation systems has grown due to the need of improving the performance of vibration isolators, which are often linear systems with linear viscous damping (LAALEJ et al. 2011). It is known that linear viscous damping reduces the forces transmitted through the isolator at the resonance frequency but increases these forces at higher frequencies. Ruzicka and Derby (1971) have studied passive isolation systems with linear stiffness and nonlinear damping. They investigated several systems, including those with hysteric damping and those in which the damping force is proportional to velocity raised to the n-th power. The case of $n = 0$ represents Coulomb damping, the case of $n = 1$ represents linear viscous damping, and the case of $n = 2$ represents quadratic damping, and so on. They have shown the usefulness of linear damping at the resonance frequency and the degradation of vibration isolation at high frequencies. Snowdon (1979) has also provided a significant review of linear isolation systems.

Ravindra and Mallik (1994) have investigated isolation systems having nonlinearity in the stiffness and the damping under both harmonic force excitation and harmonic base excitation. They have shown that for such nonlinear systems, when excited by a harmonic force, the effect of increasing the damping results in a decrease in the transmitted force at resonance and that the attenuation of forces at high frequencies is diminished, in agreement with the results presented by Ruzicka and Derby (1971). Therefore the effects of the damping in such a system are similar to those for a linear system. Transmissibility is a widely used concept to measure the performance of an isolation system. Force transmissibility is defined as the absolute value of the ratio of the excitation force to the transmitted force. Absolute displacement transmissibility is defined as absolute value of the ratio of the excitation displacement to the transmitted displacement. For a system with Coulomb damping, they have observed a strange jump in the absolute displacement transmissibility (called the jump effect). They have observed that this effect can be reduced and even eliminated by adding appropriated viscous damping.

Lang et al. (2009) have studied a single degree-of-freedom (SDOF) isolator with linear stiffness and cubic damping, applying the concept of the output frequency response function (OFRF) proposed by themselves. They showed that when this system is harmonically force-excited it can provide ideal isolation, in which only the resonant region is modified by the damping and that the behaviour of the isolator in frequency regions lower and higher than the resonance region remain unaffected, regardless of the levels of damping. This is because the relative velocity is large at frequencies near the resonance and small at frequencies higher than the resonance frequency. This is in agreement with the results obtained by Ruzicka and Derby (1971).

Milovanovic, Kovacic, and Brennan (2009) have investigated the displacement transmissibility of a system with linear stiffness and cubic damping and a system with linear-plus cubic stiffness and linear damping, both under base excitation. For the first system they have shown that in order to give a bounded response it is necessary to have a finite value of damping for each nonlinear stiffness term, this is different to that of a linear isolator where any value of damping results in a bounded response. Regarding the system with cubic damping they have found that this damping has a beneficial response in the resonance region but the performance at high frequencies is very poor.

Laalej et al. (2012) have investigated experimentally the beneficial of a cubic damper in vibration isolation. Using an active vibration isolation test rig, the authors have shown that significant benefits result from the use of cubic non-linear damping in SDOF vibration isolation systems, when force transmissibility is of interest.

Tang and Brennan (2012) have analysed the free vibration of a SDOF isolator with linear viscous damping, cubic damping and geometrically nonlinear damping in which the damper is orientated at ninety degrees to the spring. They have shown that for low levels of vibration that cubic damping is equivalent to the geometrical nonlinear damping. Further, they showed that the system with cubic damping is very poor in attenuating free vibration.

Tang and Brennan (2013) have analysed a system in which the damper is oriented at ninety degrees to the spring, excited harmonically by either a force or a base displacement. They have compared its performance with that of a linear system and with that of a system with cubic damping. In this dissertation, part of this work is reproduced in detail to compare the differences between these two systems, and the advantages of such a system compared to a linear system. Similar methods are initially employed in the analysis, but analysis based on the Fourier series on the time histories of the transmitted forces is also carried out.

1.3 Objectives

The specific objectives of this dissertation are to:

- Compare the performance of a linear vibration isolation system with the performance of a nonlinear isolation system in which the damper is orientated at ninety degrees with respect to the spring. This is done for low and high amplitude excitation, and for force and base excited systems.

- Analyse the time history and the Fourier series of the force transmitted through the nonlinear isolator to determine the behaviour of the force transmissibility at frequencies close to the resonance frequency.

1.4 Contributions

The contributions of this dissertation are as follows:

- From the study of the nonlinear system when excited with low amplitude vibration, it has been shown that the damping force depends on the square of the relative displacement and it makes the nonlinear isolator suitable for vibration isolation for low levels of excitation.

- Analytical expressions have been derived for the nonlinear isolator when excited with low amplitudes of force and base displacement (presented in Table 3.1). Such expressions show the relationship between the maximum and minimum allowable amplitudes of the excitation force and base displacement, in order to maintain a better performance of the nonlinear than that of the linear isolator at the resonance frequency. The relationship between the transmissibility, the excitation frequency and the damping ratio of the horizontal damper is also derived.

- It has been shown that the performance of the nonlinear system at high excitation frequencies is very good, performing better than the linear system for force excitation.

- When the system is excited at a high level of vibration it has been shown that the performance of the nonlinear system deteriorates because higher order harmonics are generated because of a cascading effect of nonlinear behaviour through the system.

1.5 Dissertation Outline

In chapter one a review of previous and related works is presented. Chapter 2 deals with a linear isolation system when excited by either a harmonic force or a harmonic base displacement. Here, the relation between the parameters of the system and how they affect the isolation in each case at different frequency regions is discussed. A brief section about transient, steady state and resonance frequency is also included.

In Chapter 3 the nonlinear isolation system in which the damper is orientated at ninety degree to the spring is analysed. The performance of this nonlinear system is compared with that of a linear system when the system is excited either by a harmonic force or by a harmonic displacement. In each case the system is studied for low amplitude excitation, for which the nonlinear damping force can be approximated to an equivalent viscous damping force, and for high amplitude excitation where numerical analysis is conducted.

In Chapter 4 the time histories for the force transmitted to the base at frequencies near the resonance frequency are analysed as well the frequency spectra. The forces transmitted by the spring and the damper, which sum to give the total transmitted force, are also analysed together with their frequency spectra. The force transmitted through the damper is then further analysed in detail to examine the nonlinear effects.

Chapter 5 presents the main conclusions from the study conducted in this dissertation. It includes a summary of the dissertation and proposes some further work.

2 THE LINEAR ISOLATOR

2.1 Introduction

The aim of this chapter is to review the characteristics of a single-degree-of-freedom (SDOF) linear isolator system. This is necessary so that a comparison between a linear and a nonlinear isolator can be conducted in Chapter 3. The interest in the SDOF linear isolation system is confined to the cases in which the system is harmonically excited by a force applied to the mass, and base excitation. The free vibration of the linear system has been reviewed in detail by Harris (1961), Rao (2008), Steidel (1989) and Thomson (1996), among several different authors and is not discussed in this chapter, as well as the behaviour of the system when is disturbed by a random excitation, which is discussed in Harris (1961) and Steidel (1989).

The concept of transmissibility and the way in which the system parameters affect this in different frequency regions are investigated. The results are shown in non-dimensional form with the intention of demonstrating the general features of the system instead of results based on specific values of the parameters.

2.2 The Linear Isolation System

A SDOF isolation system is composed of a rigid mass, an ideal spring and an ideal damper rigidly connected in parallel so that the system moves in the same direction as an external excitation force applied to the mass. Such a system is a simplification of reality. In this representation each constituent element has only one function, so that the resilient properties of the system are represented by the spring, the damping properties of the system are represented by the damper and all the inertia properties of the system are represented by a point mass.

The spring is assumed to be to be massless and with no damping, and the damper is assumed to be massless and without stiffness. Figure. 2.1 shows a SDOF isolation system which can be either harmonically force-excited or base-excited. Its motion is restricted to the vertical direction; $f_e(t)$ is the excitation force, $f_t(t)$ is the transmitted force, m represents the mass of the system, k is the elastic constant of the spring, c is the damping coefficient of the damper, $x(t)$ represents the mass displacement, $y(t)$ represents the base displacement, and $z(t) = x(t) - y(t)$ is the relative displacement. The system stores kinetic energy by means of the movement of mass, the potential energy of the system is stored in the spring, and the energy of the system is dissipated by the damper. The displacement variables are all time dependent; because of that it will be use a notation in which it will just appear the variables without its explicit dependence on time.

Figure 2.1 – A SDOF isolation system comprised of a rigid mass, a massless linear viscous damper and a massless linear spring. The system is excited in the vertical direction with either a harmonic force $f_e(t) = F_e \cos \omega t$ and $y(t) = 0$ or harmonic displacement by the base $y(t) = Y \cos \omega t$ and $f_e(t) = 0$, where ω is the excitation frequency is and t is time. Its movement is restricted to the vertical direction.

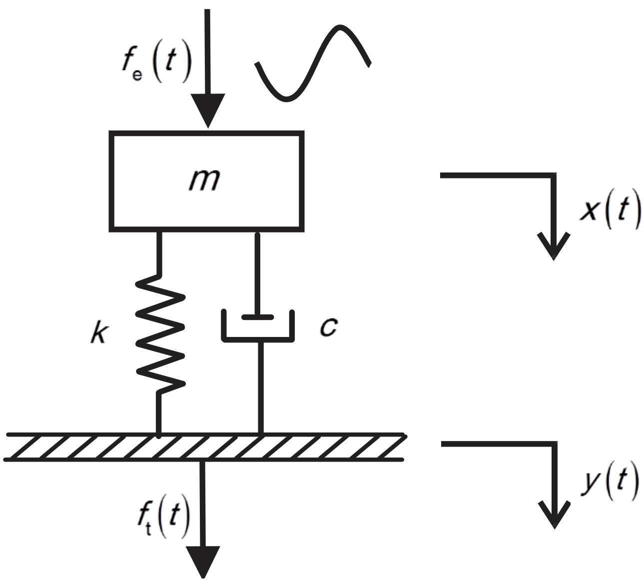

Source: Elaborated by the author

2.2.1 Equations of Motion

Most of the work in this dissertation is mainly conducted in non-dimensional variables, however some variables have dimension, mainly at the beginning of the present chapter and at the beginning of Chapter 3. To avoid confusions in this sense, it has been included a list of symbols with its dimensions in the first pages of this dissertation.

In a linear system the viscous damping force is proportional to the relative velocity between the ends of the damper and the elastic force of the spring is proportional to the relative displacement between its ends. When the system is excited by an external force, the base displacement is $y = 0$ and therefore $z = x$. The inertia of the body $f_{\mathrm{m}}(t)$, the spring force $f_{\mathrm{k}}(t)$ and the damping force $f_{\mathrm{d}}(t)$ act in opposite direction to the excitation force $f_{\mathrm{e}}(t)$. This relation between the forces on the system can be written as

$$f_{\mathrm{m}}(t) + f_{\mathrm{d}}(t) + f_{\mathrm{k}}(t) = f_{\mathrm{e}}(t) \tag{2.1}$$

The harmonic excitation force has the form $f_{\mathrm{e}}(t) = F_{\mathrm{e}} \cos \omega t$, where F_{e} is the amplitude of the force, ω is the excitation frequency and t is the time. The force due to the mass is $f_{\mathrm{m}}(t) = -m\ddot{x}$, the linear damping force is $f_{\mathrm{d}}(t) = -c\dot{x}$ and $f_{\mathrm{k}}(t) = -kx$ is the elastic force of the spring. The overdot indicates differentiation in time, so that $\dot{x}$ and $\ddot{x}$ are the mass velocity and acceleration respectively, and the negative sign indicates that inertia, damping and spring forces act in opposite direction of the relative acceleration, velocity and displacement of the mass respectively. Using Newton's second law and substituting the previous definitions of the forces in Eq. (2.1) the equation of motion of the force-excited system is given by

$$m\ddot{x} + c\dot{x} + kx = F_{\mathrm{e}} \cos \omega t \tag{2.2}$$

Note that the argument (t) is omitted here and in the remainder of this dissertation for clarity. When the system is *base-excited* there are no excitation forces $f_e = 0$ and the force due to the mass depends only on the displacement x of the mass, but the damping and stiffness forces depend on the relative displacement $z = x - y$ since the base is moving. Considering these conditions the equation of motion for the base-excited system is given by

$$m\ddot{x} + c\left(\dot{x} - \dot{y}\right) + k\left(x - y\right) = 0 \tag{2.3}$$

Subtracting $m\ddot{y}$ from both sides of Eq. (2.3), the equation of motion for the base excited system can be expressed as a function of the relative displacement

$$m\ddot{z} + c\dot{z} + kz = -m\ddot{y} \tag{2.4}$$

Equations (2.2) and (2.4) are the main equations describing the system shown in Fig. 2.1 when is force-excited and base-excited. Equation (2.3) can be rearranged so that the variables can be separated obtaining

$$m\ddot{x} + c\dot{x} + kx = c\dot{y} + k\dot{y} \tag{2.5}$$

Equation (2.5) will be useful further on when defining displacement transmissibility in Section 2.3.

2.2.2 Transient, Steady-State and Resonance Frequency

The solutions for the system described by Eqs. (2.2) and (2.4) are composed of the sum of two terms. The first term is the solution for the system when it vibrates freely, which is known as the homogenous solution and represents a *transient*. This is an oscillation at the natural frequency $\omega_n = \sqrt{k/m}$ which decays quickly in time due to the damping present in the system. The second term is the particular solution which represents the *steady-state*. This is a vibration in which the system oscillates at the excitation frequency and lasts while the excitation force is active. In a physical system, which is being excited by its base or by an external force, both kinds of vibrations are present in the system oscillation but the transient always decays after some time. The analysis on this work is based on the steady-state vibration of the systems, so that the transient is not taken in account.

A *resonant frequency* is defined as the frequency for which the system response is a maximum (Harris, 1961, p. 2-15), for the force and displacement transmissibility it can be defined as the frequency for which the transmissibility is a maximum. For low damping the resonance frequency of a system is very similar to its natural frequency ω_n. Because of this, in this work the resonance frequency is normalised by the natural frequency ω_n and the resonance frequency is assumed to be when $\omega / \omega_n = 1$.

2.3 Transmissibility for the linear isolator

The study on the linear and the nonlinear systems is conducted for two cases: 1) when the system is harmonically base-excited and 2) when the system is harmonically force-excited. This is because in vibration isolation there are two concerns: 1) to isolate a vibrating machine from its surroundings in order to reduce the transmitted vibration from the machine to a receiver and 2) isolate a delicate item of equipment from a vibrating host structure or base. Clearly the mass m represents the mass of the machine or equipment and the damper and the spring are used to reduce the transmission of movement or force. These elements together form the isolator system.

2.3.1 Force and Displacement Transmissibility

Transmissibility is one of the most used concepts to measure the performance of an isolator and is the concept used here to compare the performance between the two systems analysed on this work. Transmissibility is defined as ratio of the amplitude of the transmitted motion or force to the amplitude of the excitation motion or force (Yan B. 2007, p. 3). When the system is being harmonically force-excited ($y = 0$ and $f_e(t) = F_e \cos \omega t$) the force is transmitted through the spring and damper to the receiver, thus the transmitted force is the sum of these two forces $f_t(t) = kx + c\dot{x}$. Assuming a harmonic response and employing complex exponentials to represent the excitation force $F_e e^{j\omega t}$, the transmitted force $F_t e^{j\omega t}$ and the displacement response $x = Xe^{j\omega t}$, the amplitude of the transmitted force is

$$F_t = (k + j\omega c)X \tag{2.6}$$

where $j = \sqrt{-1}$. Following the same process Eq. (2.2) becomes

$$(k - \omega^2 m + j\omega c X) = F_e \tag{2.7}$$

Combining Eqs. (2.6) and (2.7) results in the force transmissibility given by

$$T_F = \left|\frac{F_t}{F_e}\right| = \left|\frac{k + j\omega c}{k - \omega^2 m + j\omega c}\right| \tag{2.8}$$

When the system is base-excited the transmissibility is defined as the ratio of the amplitude of the transmitted motion Y to the amplitude of the excitation motion X. Using the complex representation for the excitation displacement $x = Xe^{j\omega t}$ and the transmitted displacement $y = Ye^{j\omega t}$, in Eq. (2.5) results in the displacement transmissibility given by

$$T_D = \left|\frac{Y}{X}\right| = \left|\frac{k + j\omega c}{k - \omega^2 m + j\omega c}\right| \tag{2.9}$$

Note that force and displacement transmissibility for a linear system (Eqs. (2.8) and (2.9) respectively) are equal. To obtain a non-dimensional expression for the transmissibility, the numerator and the denominator of either Eqs. (2.8) or (2.9) are divided by k. Noting that the damping ratio $\zeta = c / 2m\omega_n$, a non-dimensional expression for the transmissibility can be determined. It is given by

$$T_F = T_D = \left|\frac{1 + j2\zeta\,\Omega}{1 - \Omega^2 + j2\zeta\,\Omega}\right| \tag{2.10}$$

where $\Omega = \omega / \omega_n$ is the non-dimensional excitation frequency. Figure. 2.2 shows force (and displacement) transmissibility for a SDOF isolation system described by Eq. (2.10) for two different damping ratios representing low and high damping. The results in Fig. 2.2 are shown in *decibels,* which is commonly used to specify transmissibility as well as other physical quantities; it is a logarithmic quantity of the ratio between two quantities, one of these being the reference quantity. The transmissibility in decibels is defined as

$$T_F(dB) = T_D(dB) = 20\log_{10}\left(\frac{F_t}{F_e}\right) \tag{2.11}$$

Figure 2.2 – Force and displacement transmissibility for a SDOF system with linear damping. Dashed line - $\zeta = 0.01$, solid line - $\zeta = 0.1$, dashed dotted line - $1/\Omega^2$, dotted line - $2\zeta_{0.01}/\Omega$, straight solid line - $2\zeta_{0.1}/\Omega$. It is possible to see that when the damping ratio is small enough - $\zeta = 0.01$ - there is a frequency region $\sqrt{2} \ll \Omega \ll \Omega_d$ in which transmissibility achieve the best case in vibration isolation for this system (dB value ref. unity).

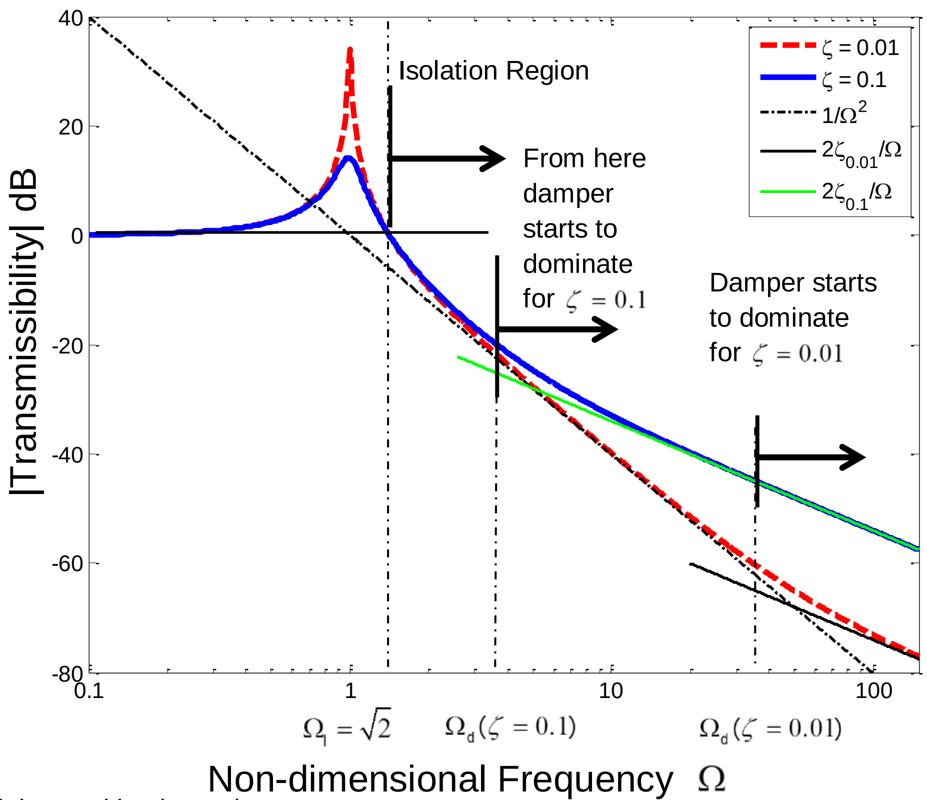

Source: Elaborated by the author

It can be seen that at frequencies lower than $\Omega_I = \sqrt{2}$, called the *isolation frequency*, the transmitted force or displacement is generally higher than the excitation force or displacement – this region is known as the amplification region. At frequencies greater than $\Omega_I = \sqrt{2}$ the transmitted force or displacement is smaller than the excitation force or displacement – this region is known as the isolation region. It also can be seen that transmissibility at frequencies close the resonance is determined by the amount of damping in the system; the larger the damping ratio the smaller the transmissibility at the resonance. The effect of viscous damping has the opposite effect in the isolation region. Increasing the damping ratio results in a detrimental effect on the performance of the isolator, causing an increase in the transmissibility in this region. There is a compromise in the choice of damping between good control at resonance and good control at high frequencies (YAN B. 2007, p. 5). Finally Fig. 2.2 shows that at very low frequencies $T = 1$, transmitted force or displacement is equal to that of the excitation, which in decibels notation corresponds to $T\left(dB\right) = 0$.

Recalling that the numerator of Eq. (2.10) is the transmitted force and this force is composed of the sum of the damping and the spring forces, it can be seen that the term $j2\zeta\,\Omega$ in the numerator is related to the damping force and the term 1 in the numerator is related to the spring force.

2.3.2 Transmissibility analysis for the linear system

Some analysis about transmissibility can be conducted by means of Eq. (2.10). It is possible to find the frequency at which the force (or displacement) through the damper starts to dominate the transmissibility. For this to happen the damping force must to be equal to the force of the spring in the numerator of Eq. (2.10) then $1 = j2\zeta\,\Omega$ and the frequency at which the force through the damper starts to dominate the transmissibility is $\Omega_d = 1/2\zeta$. To determine the transmissibility peak at the resonance frequency, $\Omega = 1$ is set in Eq. (2.10) and the largest terms remaining are taken to obtain the value of transmissibility at resonance

$$\left|T_{\mathrm{F}}\right|_{\Omega=1} = \left|T_{\mathrm{D}}\right|_{\Omega=1} \approx \frac{1}{2\zeta} \tag{2.12}$$

From Eq. (2.12) can be seen what have been showed in Fig. 2.2, that an increase in the damping results in a decrease in the transmissibility at the resonance frequency. To determine the behaviour of transmissibility at high excitation frequencies, $\Omega \gg \Omega_{\mathrm{d}}$ is set in Eq. (2.10) and then the largest term in the numerator and in the denominator are taken to obtain

$$\left|T_{\mathrm{F}}\right|_{\Omega\gg1} = \left|T_{\mathrm{D}}\right|_{\Omega\gg1} = \frac{2\zeta}{\Omega} \tag{2.13}$$

From Eq. (2.13) can be seen that far the resonance frequency an increase in damping brings to an unfavourable effect increasing the transmissibility at this frequencies. If the damping is low, which is the case when $\zeta = 0.01$ so that the frequency at which damping force starts to dominate the transmissibility become very high compared with the isolation frequency $\Omega_{\mathrm{d}} \gg \sqrt{2}$ the force through the spring take account on transmissibility and then there is a frequency region $\sqrt{2} \ll \Omega \ll \Omega_{\mathrm{d}}$ where

$$\left|T_{\mathrm{F}}\right| = \left|T_{\mathrm{D}}\right| = \frac{1}{\Omega^2} \tag{2.14}$$

which is the best case which can be achieved in transmissibility for a SDOF system (TANG; BRENAN, 2013). With low damping transmissibility decreases at a rate of 40dB per decade whilst with high damping transmissibility decrease at a rate of 20 dB per decade as showed in Fig 2.2.

2.4 Conclusions

In this chapter the most important features of a SDOF isolation system when it is either excited by a harmonic force or is base-excited have been discussed. The concept of transmissibility has been defined and used to measure the performance of the system. This has provided a benchmark by which the performance of a nonlinear isolator can be compared in Chapter 3. For the linear system it has been shown that there are three regions in the transmissibility curve; the amplification region for frequencies below $\Omega_I = \sqrt{2}$, the region at which the transmissibility is mainly dominated by the spring and the region at which the transmissibility is mainly dominated by the damper. The last two regions are in the isolation region at frequencies above Ω_I. It has been shown that damping in the isolator has a beneficial effect at frequencies close to the resonance frequency, but it has a detrimental effect at high frequencies, where it increases the transmissibility.

3 NONLINEAR DAMPING ISOLATOR

3.1 Introduction

In Chapter 2 a SDOF isolation system has been studied. The main equations describing the system when it is force and base excited has been shown. The concept of transmissibility has been revised at different excitation frequencies and presented as a mean by which the performance of the linear system can be compared. In this chapter a SDOF system with a nonlinear damper is analysed. Its performance is determined and the way in which the nonlinearity affects the internal forces is investigated. To determine the performance of the system its force and displacement vibration transmissibility are compared with that of a linear system under harmonic force and harmonic base excitation. The study is conducted for both small amplitude excitation, as it is possible to use analytical approximated expressions, and for high amplitude excitation which is based on numerical simulations.

This system is similar to the SDOF linear system described in Chapter 2. It is also composed of a mass, a linear spring and a linear damper; but its damper is placed so that it forms a 90º angle with the spring, as shown in Fig. 3.1. All the nonlinear characteristics of the isolator are due to this geometrical configuration.

The system is excited in the direction of the spring and perpendicular to the damper with either a harmonic force, when investigating the force transmissibility, or harmonic displacement by the base, when investigating the displacement transmissibility.

Tang and Brennan (2013) analysed this system with the purpose of investigating the advantages of such a damper configuration for force and displacement transmissibility. Here, part of this work is reproduced in detail to compare its differences and advantages with that of a linear system, sometimes using similar methods as employed by them and sometimes using other methods to confirm their results.

Figure 3.1 – A SDOF system with damper oriented perpendicular to the spring (Horizontal damper system). The system is excited in the vertical direction with either a harmonic force $f_e(t) = F_e \cos \omega t$ and $y(t) = 0$ or harmonic displacement by the base $y(t) = Y \cos \omega t$ and $f_e(t) = 0$, where ω is the excitation frequency and t is time. Its movement is restricted to the vertical direction.

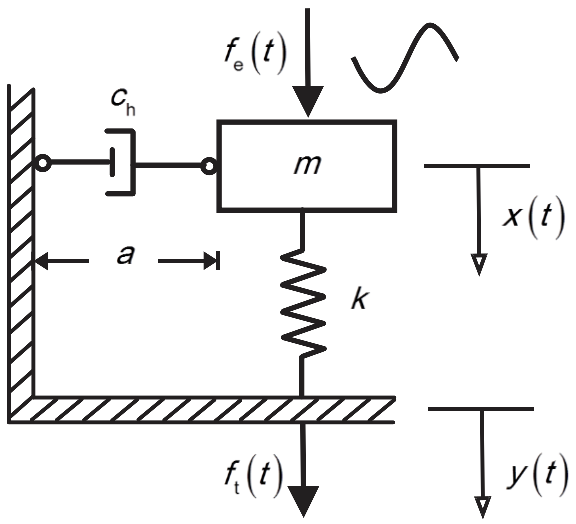

Source: Elaborated by the author

3.2 Equations of motion

As the nonlinear characteristics of the system are due only to the geometric configuration of the damper, it is necessary to determine the form of the damping force in the direction of motion, in order to determine the equation of motion for the system.

Figure 3.2 shows a free-body diagram of the damper. It can be seen that the damping force in the vertical direction is given by $f_d(t) = F_h \sin\theta$ and the damper length in any position by $h = \sqrt{a^2 + z^2}$, where $f_h(t)$ is the force produced by the horizontal linear damper, c_h is the horizontal linear damping coefficient, a is the original damper length and $z = x - y$ is the relative displacement between the mass

Figure 3.2 – Triangle formed by the horizontal damper in two different positions. The damper length is a, the hypotenuse h corresponds to horizontal damper length in any position; θ is the angle formed by the damper and the horizontal line, the relative displacement between the mass and the base is z, c_h is the horizontal linear damping coefficient, the horizontal linear damping force is $f_h(t)$ and the nonlinear damping force produced by the horizontal damper in the vertical direction is $f_d(t)$.

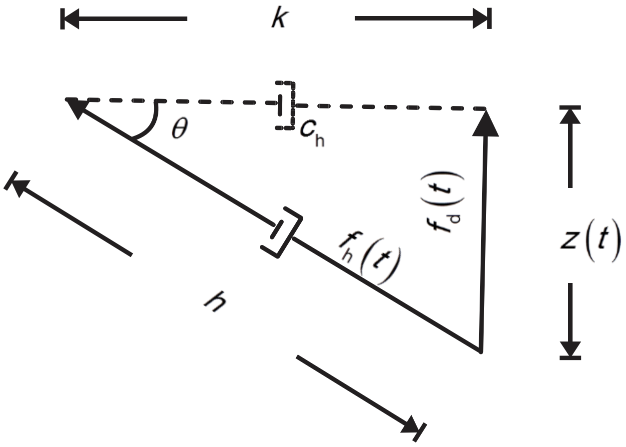

Source: Elaborated by the author

and the base; when the system is force-excited, the base is stationary, so $y = 0$, and then $z = x$ (see Fig. 3.1).

According to Fig. 3.2 $f_d(t) = f_h(t)\sin\theta$, expressing $f_h(t)$ as the multiplication of the relative velocity $\dot{z}$ and a damping coefficient which takes into account the geometric properties of the damper in any position, and representing $\sin\theta$ in terms of z and a, a nonlinear expression of the damping force is obtained

$$f_d(t) = c_h \frac{z^2}{a^2 + z^2} \dot{z} \tag{3.1}$$

Note that unlike a linear damping force the nonlinear damping force depends upon the amplitude of the relative displacement and not just upon the relative velocity, hence the system nonlinearity is caused by this dependence. As discussed by Tang and Brennan (2013), this kind of damping could be useful in situations in which large damping is required for a large relative displacement, for example at resonance, and low damping is required for a low relative displacement, for example well-above the resonance frequency.

As the system is forced by $f_{\mathrm{e}}(t)$, the mass, or inertia, resists the change in movement and then acts in opposite direction of $f_{\mathrm{e}}(t)$; the stiffness and damping forces act against the movement too. These relations can be written as

$$f_{\mathrm{m}}(t)+f_{\mathrm{d}}(t)+f_{\mathrm{k}}(t)=f_{\mathrm{e}}(t) \tag{3.2}$$

where $f_{\mathrm{m}}(t)$ is the force due to the mass, $f_{\mathrm{d}}(t)$ is the damping force in the vertical direction, $f_{\mathrm{k}}(t)$ is the linear spring force. When the system is force-excited ($y=0$), the harmonic excitation force is given by $f_{\mathrm{e}}(t)=F_{\mathrm{e}}\cos\omega t$ and the stiffness and damping forces are given by $f_{\mathrm{k}}(t)=-kx$ and $f_{\mathrm{d}}(t)=-c_{\mathrm{h}}\dot{x}$ respectively. Using Newton's second law and substituting the previous expressions for each force into Eq. (3.2) gives the equation of motion for the force-excited system

$$m\ddot{x}+c_{\mathrm{h}}\frac{x^2}{a^2+x^2}\dot{x}+kx=F_{\mathrm{e}}\cos\omega t \tag{3.3}$$

As discussed in Chapter 2, when the system is base-excited ($f_{\mathrm{e}}(t)=0$) the force due to the mass depends only on the displacement of the mass x, but the damping and stiffness forces depend on the relative displacement $z=x-y$. The corresponding equation of motion is then given by

$$m\ddot{x}+c_{\mathrm{h}}\frac{z^2}{a^2+z^2}\dot{z}+kz=0 \tag{3.4}$$

Subtracting $m\ddot{y}$ from both sides of the Eq. (3.4), the equation of motion for the base-excited system becomes

$$m\ddot{z}+c_{\mathrm{h}}\frac{z^2}{a^2+z^2}\dot{z}+kz=-m\ddot{y} \tag{3.5}$$

Eqs (3.3) and (3.5) are the key equations describing the system shown in Fig. 3.1. Comparing Eqs. (3.3) and (3.5) with Eqs. (2.2) and (2.4), which are the main equations describing the linear system, it can be seen that the difference is in the nonlinearity present in the damping force of the nonlinear system. Eqs. (3.3) and (3.5) can be solved using numerical methods, which is done in Section 3.4. However some analysis is first conducted for low amplitudes of excitation. To do this some approximations for the damping force have to be made.

3.3 Low Amplitude Excitation Study

When the relative displacement $z < 0.2a$ the term z^2 in the numerator of Eq. (3.1) is small compared with a^2 and can be neglected and this gives a simpler form of the damping force, which is given by

$$f_\mathrm{d} = c_\mathrm{h} \frac{z^2}{a^2} \dot{z} \tag{3.6}$$

The validity of this approximation is investigated by comparing the energy dissipated by a damper with the actual damping force Eq. (3.1) and a damper with the approximate damping force Eq. (3.6).

3.3.1 Energy Dissipated by a Damping Force

In general, the energy dissipated by a damping force for a damper alone, such as that shown in Fig. 3.3, is given by the work done by the damping force (RUZICKA; DERBY, 1971). Assuming a harmonic relative displacement $z = Z \sin \omega t$, the energy dissipated by the damping is four times the work done by the damping force over a quarter of cycle of vibration, thus,

$$E = 4 \int_0^{\pi/2\omega} f_\mathrm{d} \dot{z} dt \tag{3.7}$$

Figure 3.3 – Schematic representation of a damper with equivalent viscous damping excited by a harmonic force.

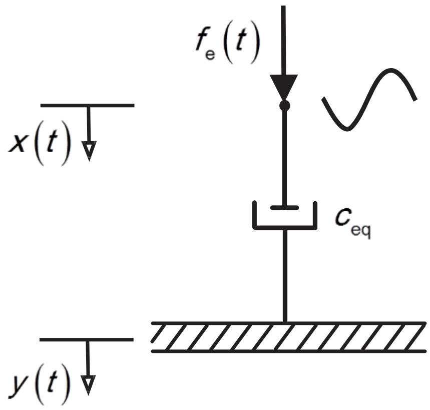

Source: Elaborated by the author

Substituting for $\dot{z}$ together with f_d given in Eq. (3.1) into Eq. (3.7), gives after some manipulation, the energy dissipated by the damping force

$$E = 4c_h\omega^2 Z^4 \int_0^{\pi/2\omega} \left(\frac{\sin^2(\omega t)\cos^2(\omega t)}{a^2 + Z^2\sin^2(\omega t)} \right) dt \tag{3.8}$$

In order to obtain the approximate expression for the energy dissipated by the damping $\dot{z}$ and Eq. (3.6) are substituting in Eq. (3.7), resulting

$$E_{\text{Approx.}} = 4c_h\omega^2 \frac{Z^4}{a^2} \int_0^{\pi/2\omega} \left(\cos^2(\omega t) - \cos(\omega t)\cos^3(\omega t) \right) dt \tag{3.9}$$

Using the trigonometric identity

$$\cos^3 \omega t = \frac{3\cos\omega t}{4} + \frac{\cos 3\omega t}{4} \tag{3.10}$$

It can be seen that for an excitation at frequency ω there is a response at this frequency and at three times this frequency. If the response at only the excitation frequency is considered (note that this is three times that of the third harmonic), then Eq. (3.9) simplifies to

$$E_{\text{approx}} = \frac{\pi c_h \omega Z^4}{4a^2} \tag{3.11}$$

To compare the approximate energy dissipated by the damper given by Eq. (3.11) and the actual energy dissipated given by Eq. (3.8), they are divided by the energy dissipated by a linear damper $E_{\mathrm{l}} = \pi c \omega Z^2$ (RAO, 2008, p. 70).

Setting $c_{\mathrm{h}} = c$, where c is the linear viscous damping, and dividing Eqs. (3.8) and (3.11) by E_{l}, the normalised energy dissipated, which includes all the harmonics, and the normalised energy approximated, which includes just the harmonic at the excitation frequency, are respectively given by

$$\hat{E} = \frac{E}{E_{\mathrm{l}}} = \frac{4\hat{Z}^2}{\pi} \int_0^{\pi/2} \left(\frac{\sin^2(\omega t)\cos^2(\omega t)}{1 + Z^2 \sin^2(\omega t)} \right) d(\omega t) \tag{3.12}$$

and

$$\hat{E}_{\text{Approx.}} = \frac{\hat{Z}^2}{4} \tag{3.13}$$

where $\hat{Z} = Z / a$. The expression for the actual damper given by Eq. (3.12) is integrated numerically to give the normalised energy dissipated as a function of $\hat{Z}$. Figure 3.4 shows the normalised energy dissipated by the actual and the approximate damping forces, given by Eqs. (3.12) and (3.13), as a function of the relative displacement. It can be seen that both have similar behaviour - that of a parabola, as they are dependent on $\hat{Z}^2$, and that the lines begin to separate at the point $\hat{Z} \approx 0.2$. At this point the maximum error in the approximation for is only about 2%. Figure 3.5 shows the ratio of energy dissipated calculated using the approximate expression to the actual energy dissipated in one cycle as functions of $\hat{Z}$. It can be seen that the energy calculated with the approximate expression is similar to the energy calculated using the actual expression for the damping force. Thus, it can be concluded that Eq. (3.6) is a good approximation to the damping force Eq. (3.1) for values of $\left| z/a \right| < 0.2$ as discussed by Tang and Brennan (2013).

Figure 3.4 – Non-dimensional energy dissipated. Solid line, energy calculated using the actual damping force; dashed line, energy calculated using the approximated damping force.

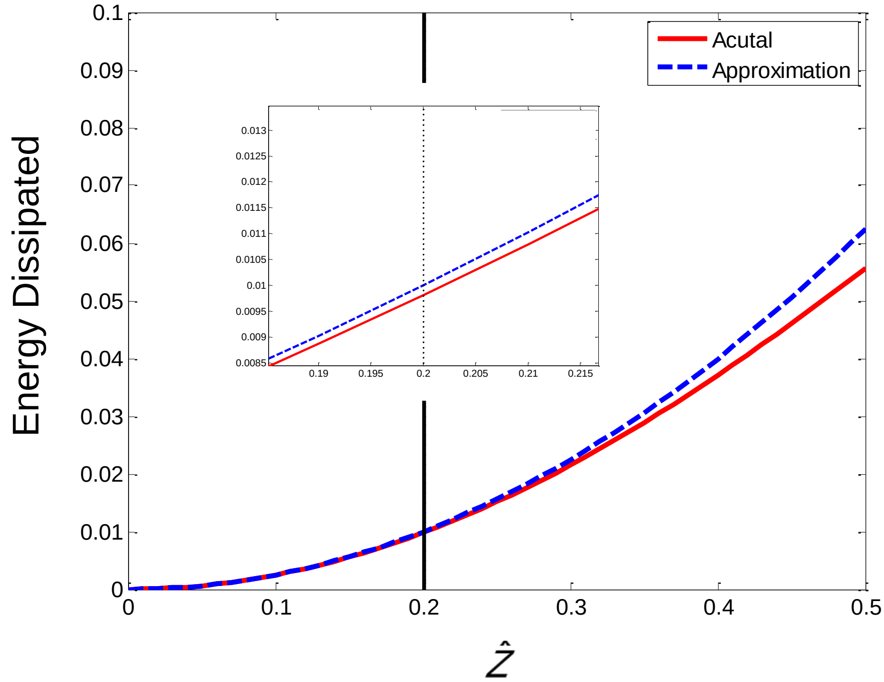

Source: Elaborated by the author

Figure 3.5 –Ratio of actual energy dissipated to approximated energy dissipated. Solid line, energy ratio calculated using the approximate damping force; dashed line, energy ratio calculated using the actual damping force.

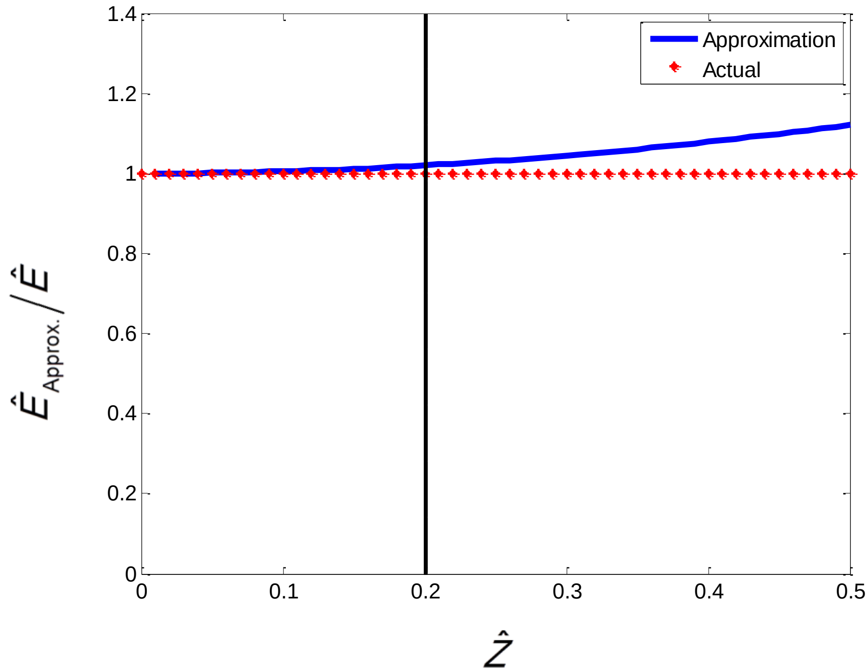

Source: Elaborated by the author

3.3.2 Equivalent Viscous Damping

It is possible to approximate the nonlinear damping forces Eqs. (3.1) and (3.6) to *equivalent linear viscous damping forces* and thus represent the horizontal damper system shown in Fig. 3.1 as the equivalent linear system shown in Fig. 3.6, by employing the concept of *equivalent viscous damping*, such that Eqs. (3.1) and (3.6) could be written as the multiplication of the equivalent damping coefficient and the relative velocity $f_{\mathrm{d}} = c_{\mathrm{eq}}\dot{z}$.

Figure 3.6 – Schematic representation of a SDOF system with equivalent linear viscous damping force. The system is excited in the vertical direction with either harmonic force f_{e} and $y = 0$ or harmonic displacement by the base y and $f_{\mathrm{e}} = 0$. Its movement is restricted to the vertical direction.

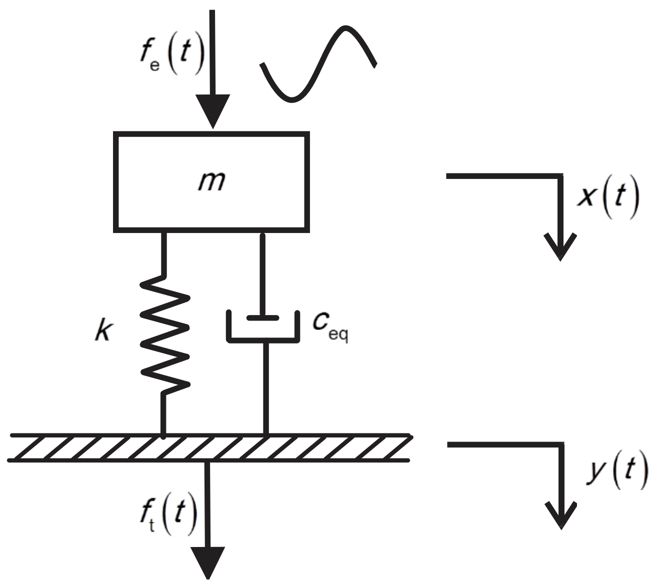

Source: Elaborated by the author

As the interest in this section is the low amplitude transmissibility the approximate damping force us used to obtain c_{eq}. A similar process can be conducted to obtain c_{eq} for the actual damping force, however below it is shown that there is an easier way to obtain it. According to Ruzicka and Derby (1971) to achieve equivalence, between a nonlinear and a linear viscous damper, the energy dissipated by the nonlinear damper in one vibration cycle should be equal to the energy dissipated by a linear viscous damper for the same harmonic relative displacement.

It was shown in the last subsection that the damper with the approximate damping force of Eq. (3.6), is valid for relative displacement values $\left| z/a \right| < 0.2$. The equivalent viscous damping coefficient c_{eq} can be determined by equating the energy dissipated per cycle by the nonlinear damping element Eq. (3.11) to that dissipated by the horizontal viscous damper $c_{\mathrm{h}}\pi\omega Z^4 / 4a^2 = c_{\mathrm{eq}}\pi\omega Z^2$ (RUZICKA; DERBY, 1971), solving for c_{eq} gives

$$c_{\mathrm{eq}} = \frac{1}{4} c_{\mathrm{h}} \frac{\left|Z\right|^2}{a^2} = c_{\mathrm{h}} \frac{\left|\hat{Z}\right|^2}{4} \tag{3.14}$$

which is the same as multiplying Eq. (3.13) by the horizontal viscous damping coefficient c_{h}. So to obtain c_{eq} for the actual damping force it is necessary simply multiply Eq. (3.12) by c_{h}, as c_{h} is a constant which multiplies both Eqs. (3.12) and (3.13). Figure (3.4) can then be thought of as representing the behaviour of the equivalent viscous damping coefficients as functions of $\hat{Z}$, for the actual and the approximate damping forces and Fig. (3.5) as representing its ratio as function of $\hat{Z}$.
Now, it is possible to write the equation of motion for the harmonic force-excited system Eq. (3.3) as

$$m\ddot{x} + c_{\mathrm{eq}}\dot{x} + kx = F_{\mathrm{e}} \cos \omega t \tag{3.15}$$

and the equation of motion for the harmonically base-excited system Eq. (3.5), as

$$m\ddot{z} + c_{\mathrm{eq}}\dot{z} + kz = -\omega^2 mY \cos \omega t \tag{3.16}$$

where Y is the base displacement amplitude. Therefore the nonlinear system of Fig. 3.1 can be represented as the equivalent system in Fig. 3.6.

Equations. (3.15) and (3.16) can be expressed as dimensionless equations by using the *damping ratio* and by defining some non-dimensional variables. The linear damping ratio ζ was defined in Chapter 2 as the ratio of the damping coefficient c to the critical damping of the system, which is given by $2m\omega_{\mathrm{n}}$, where ω_{n} is the natural frequency of the system. As c_{h} is the horizontal viscous damping coefficient,

$\zeta_h = \dfrac{c_h}{2m\omega_n}$ represents the horizontal damping ratio. From Eq. (3.14) and the previous the definitions, the equivalent damping ratio for the approximate system can be written as

$$\zeta_{eq} = \frac{1}{4}\zeta_h \left|\hat{Z}\right|^2 \tag{3.17}$$

Dividing Eqs. (3.15) and (3.16) by ka and using the non-dimensional force $\hat{F}_e = F_e / a$, the amplitude of base displacement $\hat{Y} = Y / a$, the frequency $\Omega = \omega / \omega_n$, the mass displacement $\hat{x} = x / a$, the relative displacement $\hat{z} = z / a$, and the non-dimensional mass and relative velocities $\hat{z}' = \dot{z} / \omega_n a$, $\hat{x}' = \dot{x} / \omega_n a$, and accelerations $\hat{z}'' = \ddot{z} / \omega_n^2 a$, $\hat{x}' = \ddot{x} / \omega_n^2 a$, which are obtained by differentiating $\hat{x}$ and $\hat{z}$ in the non-dimensional time $\tau = \omega_n t$, they can be written as

$$\hat{x}'' + 2\zeta_{eq}\hat{x}' + \hat{x} = \hat{F}_e \cos\Omega\tau \tag{3.18}$$

$$\hat{z}'' + 2\zeta_{eq}\hat{z}' + \hat{z} = \Omega^2\hat{Y} \cos\Omega\tau \tag{3.19}$$

which are the general non-dimensional equations of motion for the harmonic force-excited and the harmonic base-excited systems respectively. Note that ζ_{eq} does not necessarily come from the approximated expression to the damping force Eq. (3.17) but can come from the actual damping force.

3.3.3 Transmissibility Equations for Low Amplitude Excitation

Force and displacement transmissibility were defined in Section 2.3 of Chapter 2 as the ratio between the transmitted force to the excitation force and the transmitted displacement to the base excitation, respectively. It was shown that in the linear case force transmissibility is equals to displacement transmissibility. The force is transmitted through the damper and the spring, however for the nonlinear system the damping force has a different form, which leads to a different damping ratio. The excitation force $\hat{F}_\mathrm{e}\cos\Omega\tau$ can be written as the real part of a complex number $\hat{F}_\mathrm{e}e^{j\Omega\tau}$ by employing the complex exponential, since $e^{j\Omega\tau} = \cos\Omega\tau + j\sin\Omega\tau$. The use of complex exponentials to represent the force makes the calculations easier because the algebra is simpler. In the same way the mass, base and relative displacements can be represented as complex numbers $\hat{x} = \hat{X}e^{j\Omega\tau}$, $y = \hat{Y}e^{j\Omega\tau}$ and $\hat{z} = \hat{Z}e^{j\Omega\tau}$ respectively. Substituting the complex forms of the excitation force and displacements, and Eq. (3.17) in Eq. (2.10) from Chapter 2, the force and displacement transmissibility for the nonlinear system are given by

$$T_\mathrm{F} = \frac{1 + j\frac{1}{2}\zeta_\mathrm{h}\left|\hat{X}\right|^2\Omega}{1 - \Omega^2 + j\frac{1}{2}\zeta_\mathrm{h}\left|\hat{X}\right|^2\Omega} \tag{3.20}$$

$$T_\mathrm{D} = \frac{1 + j\frac{1}{2}\zeta_\mathrm{h}\left|\hat{Z}\right|^2\Omega}{1 - \Omega^2 + j\frac{1}{2}\zeta_\mathrm{h}\left|\hat{Z}\right|^2\Omega} \tag{3.21}$$

Note that unlike the linear system, for the nonlinear damper system the force and displacement transmissibility are not the same. This is because for the nonlinear system the damper force depends on the square of the relative displacement which is $\hat{Z} = \hat{X} - \hat{Y}$ for the base excited system and $\hat{Z} = \hat{X}$ for the force excited system.

In order to obtain the transmissibility at each frequency of excitation it is necessary to know the displacement and relative displacement at this frequency. These are given by

$$\hat{X} = \frac{\hat{F}_e}{1 - \Omega^2 + j\frac{1}{2}\zeta_\mathrm{h}\left|\hat{X}\right|^2\Omega} \tag{3.22}$$

$$\hat{Z} = \frac{\Omega^2\hat{Y}}{1 - \Omega^2 + j\frac{1}{2}\zeta_\mathrm{h}\left|\hat{Z}\right|^2\Omega} \tag{3.23}$$

In Eqs. (3.22) and (3.23) the unknown variable is a function of itself. Tang and Brennan (2013) used the harmonic balance method (HBM) to determine $\hat{X}$ and $\hat{Z}$

and have suggested that Eqs. (3.22) and (3.23) can be solved iteratively. Here, another solution method is used.

3.3.4 Solution of Transmissibility Equations (Low Amplitude Excitation)

Note that the transmissibilities given in Eqs. (3.20) and (3.21) are not dependent on the complex displacement amplitude but the absolute value of displacement amplitude and that Eqs. (3.22) and (3.23) are complex functions and therefore they can be represented in the form $\psi = \alpha + j\beta$, where ψ is a complex number, α is the real part and β the imaginary part of ψ. It is thus possible to find $\left|\hat{X}\right|$ and $\left|\hat{Z}\right|$ by analogy to finding the absolute value of a complex number, that is $\left|\psi\right| = \sqrt{\psi^{*}\psi}$, where ψ^{*} is the conjugate of ψ.

Multiplying the right side of Eq. (3.22) by its denominator and then separating the result in its real and imaginary parts leads to

$$\hat{X} = \left(\frac{\hat{F}_{e}\left(1-\Omega^{2}\right)}{\left(1-\Omega^{2}\right)^{2} + \left(\frac{1}{2}\zeta_{h}\left|\hat{X}\right|^{2}\Omega\right)^{2}} \right) - j\left(\frac{\hat{F}_{e}\frac{1}{2}\zeta_{h}\left|\hat{X}\right|^{2}\Omega}{\left(1-\Omega^{2}\right)^{2} + \left(\frac{1}{2}\zeta_{h}\left|\hat{X}\right|^{2}\Omega\right)^{2}} \right) \tag{3.24}$$

For the force-excited system to obtain $\left|\hat{X}\right|$ it is just necessary to multiply $\hat{X}$ by its conjugate and take the root square of the result, which can be written as

$$\left|\hat{X}\right| - \left[\left(\frac{\hat{F}_{e}\left(1-\Omega^{2}\right)}{\left(1-\Omega^{2}\right)^{2} + \left(\frac{1}{2}\zeta_{h}\left|\hat{X}\right|^{2}\Omega\right)^{2}} \right)^{2} + \left(\frac{\hat{F}_{e}\frac{1}{2}\zeta_{h}\left|\hat{X}\right|^{2}\Omega}{\left(1-\Omega^{2}\right)^{2} + \left(\frac{1}{2}\zeta_{h}\left|\hat{X}\right|^{2}\Omega\right)^{2}} \right)^{2} \right]^{1/2} = 0 \tag{3.25}$$

One way to determine the value of $\left|\hat{X}\right|$ for every frequency Ω is to search for the value of $\left|\hat{X}\right|$ for which Eq. (3.25) is satisfied. Once a value of $\left|\hat{X}\right|$ is obtained this is used in Eq. (3.20) to determine a value of transmissibility for every Ω and then the process is repeated for the next frequency Ω. Such a procedure is used for the base-excited system as well, and the equation from which $|\hat{Z}|$ is obtained is

$$|\hat{Z}|-\left[\left(\frac{\Omega^2\hat{Y}\left(1-\Omega^2\right)}{\left(1-\Omega^2\right)^2+\left(\frac{1}{2}\zeta_h|\hat{Z}|^2\Omega\right)^2}\right)^2+\left(\frac{\hat{Y}\frac{1}{2}\zeta_h|\hat{Z}|^2\Omega}{\left(1-\Omega^2\right)^2+\left(\frac{1}{2}\zeta_h|\hat{Z}|^2\Omega\right)^2}\right)^2\right]^{1/2}=0 \qquad (3.26)$$

In Fig. 3.7 are shown the force and displacement transmissibilities for the nonlinear isolator system when $\hat{F}_e=0.4\zeta$ and $\hat{Y}=0.4\zeta$ respectively with $\zeta_h=10$,

Figure 3.7 – Force and displacement transmissibility when $\hat{F}_e=0.4\zeta$ and $\hat{Y}=0.4\zeta$ respectively for the nonlinear isolator system with $\zeta_h=10$. Solid line - displacement transmissibility, dashed line - linear isolator with $\zeta=0.1$, dotted line - force transmissibility, dashed dotted line: $1/\Omega^2$ (dB value ref. unity)

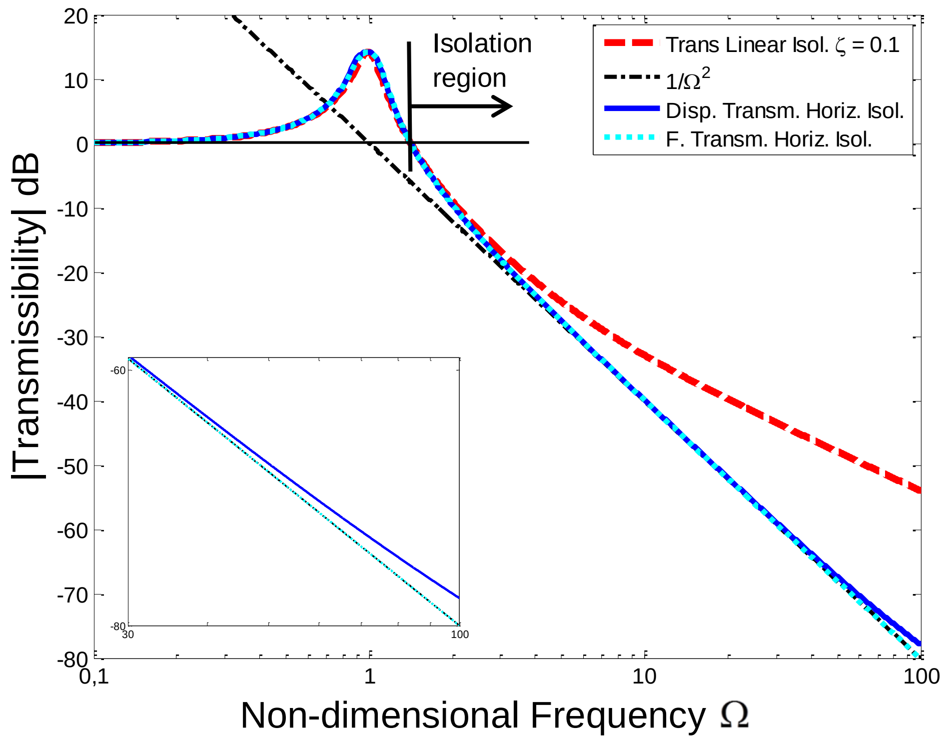

Source: Elaborated by the author

obtained using the method described above. The transmissibility of a linear isolator with $\zeta = 0.1$ is also shown for comparison. These results are similar to those presented by Tang and Brennan (2013) who used the HBM to obtain their results.

3.3.5 Transmissibility Analysis (Low Amplitude Excitation)

Some analysis can be conducted on Eqs. (3.20), (3.21), (3.22) and (3.23) with the purpose of predicting the force and displacement transmissibilities in the different frequency regions for displacement amplitudes less than or equal to $0.2a$. To determine the behaviour of transmissibility for the harmonic force-excited system for high excitation frequencies, $\Omega \gg 1$ in Eq. (3.22) is considered and then the largest terms in the numerator and in the denominator are taken to give $\left|\hat{X}\right|_{\max\{\Omega\gg1\}} = \hat{F}_{\mathrm{e}} / \Omega^2$. Substituting this result in Eq. (3.20) and taking the largest terms yields

$$\left|T_{\mathrm{F}}\right|_{\Omega\gg1} \approx \left|\frac{1 + j\dfrac{1}{2}\zeta_{\mathrm{h}}\dfrac{\hat{F}_{\mathrm{e}}^{2}}{\Omega^3}}{1 - \Omega^2 + j\dfrac{1}{2}\zeta_{\mathrm{h}}\dfrac{\hat{F}_{\mathrm{e}}^{2}}{\Omega^3}}\right| \approx \frac{1}{\Omega^2} \tag{3.27}$$

This results shows that at high frequencies the nonlinear isolator is very effective as the displacement amplitude does not depend on damping. Thus, the force through the damper become practically zero at high frequencies compared with the force through the spring and then the system behaves as it were undamped, which is the best that can be achieved for a SDOF system (see Fig. 3.7).

For the resonance region $\Omega = 1$, $\left|\hat{X}\right|_{\Omega=1} = \left(2\hat{F}_{\mathrm{e}} / \zeta_{\mathrm{h}}\right)^{1/3}$, and the transmissibility at resonance is given by

$$\left|T_{\mathrm{F}}\right|_{\Omega=1} \approx \sqrt[3]{2 / \zeta_{\mathrm{h}}\hat{F}_{\mathrm{e}}^{2}} \tag{3.28}$$

In order to maintain the transmissibility peak at resonance of the nonlinear isolator equal to or less than that of the linear isolator, the inequality

$\left(2/\zeta_{\mathrm{h}}\hat{F}_{\mathrm{e}}^{\,2}\right)^{1/3} \leq 1/2\zeta$ must be satisfied, which means that to achieve this $\hat{F}_{\mathrm{e}} \geq 4\sqrt{\left(\zeta^{3}/\zeta_{\mathrm{h}}\right)}$. That is, if the excitation force is less than this value the nonlinear isolator peak at resonance will be greater than the resonance peak of the linear system. Consequently the performance will be worse than that of the linear isolator. This is because the damping force produced by the horizontal damper is large when the relative displacement is large, and the fact that the isolator behaves as if it is undamped at high frequencies is because the damping force is small when the relative displacement is small.

According to Eq. (3.28), and what has been mentioned previously, the resonance peak of the force transmissibility for the nonlinear isolator will decrease as the excitation force $\hat{F}_{e}$ increases. This is a desirable effect, but it should be noted that this is valid only for displacement values less than $0.2a$. Taking into account this restriction and setting $\Omega = 1$ on Eq. (3.22), a limit on the excitation force is found to be $\hat{F}_{e} \leq \zeta_{h}/250$.

A similar procedure is conducted when the isolator is harmonically base-excited. For high frequencies the upper limit of the relative displacement $\left|\hat{Z}\right|_{\max\{\Omega\gg 1\}} = \hat{Y}$ is found and then the displacement transmissibility becomes

$$\left|T_{\mathrm{D}}\right|_{\Omega\gg 1} \approx \left|\frac{1+j\dfrac{1}{2}\zeta_{\mathrm{h}}\hat{Y}^{2}\Omega}{1-\Omega^{2}+j\dfrac{1}{2}\zeta_{\mathrm{h}}\hat{Y}^{2}\Omega}\right| \approx \frac{\zeta_{\mathrm{h}}\hat{Y}^{2}}{2\Omega} \tag{3.29}$$

Note that at high frequencies there is a detrimental effect on the displacement transmissibility for the base-excited isolator when compared with the force-excited isolator as shown in Fig. 3.7. This effect is similar to that produced by a linear isolator where the force and displacement transmissibilities are proportional to $1/\Omega$. Equating the terms in the numerator of Eq. (3.29) the frequency value at which the force through the damper starts to dominate the transmissibility in the nonlinear isolator can be found, this is given by $\Omega_{\mathrm{d}} = 2/\zeta_{\mathrm{h}}\hat{Y}^{2}$. At frequencies lower or equal to Ω_{d} but inside the isolation region, it is the force through the spring which mainly dominates the transmissibility and then for these values the transmissibility is proportional to $1/\Omega^2$. In order to obtain a better performance than the linear isolator, Ω_d for the nonlinear isolator should be higher than Ω_d for the linear isolator, that is $2/\zeta_h\hat{Y}^2 > 1/2\zeta$ and from this provided that $\hat{Y} < 2\sqrt{(\zeta/\zeta_h)}$ the frequency range for which the displacement transmissibility is proportional to $1/\Omega^2$ will be extended and will be larger than the corresponding range for the linear isolator.

At the resonance frequency, and from Eq. (3.23), the limit for the relative displacement is $\left|\hat{Z}\right|_{\Omega=1} = \left(2\hat{Y}/\zeta_h\right)^{1/3}$, substituting this value into Eq. (3.21) and

Table 3.1 Important values for the linear and the nonlinear horizontal damper isolators valid for displacement amplitudes less or equal to $0.2a$.

	Force-excited		Base-excited	
	Linear viscous Damper	Horizontal linear viscous damping	Linear viscous Damper	Horizontal linear viscous damping
Amplitude of relative displacement at resonance $\left\|\hat{X}\right\|_{\Omega=1}$ **or** $\left\|\hat{Z}\right\|_{\Omega=1}$	$\hat{F}_e/2\zeta$	$\left(2\hat{F}_e/\zeta_h\right)^{1/3}$	$\hat{Y}/2\zeta$	$\left(2\hat{Y}/\zeta_h\right)^{1/3}$
Amplitude of transmissibility at resonance $\left\|T_F\right\|_{\Omega=1}$ **or** $\left\|T_D\right\|_{\Omega=1}$	$1/2\zeta$	$\left(2/\zeta_h\hat{F}_e^2\right)^{1/3}$	$1/2\zeta$	$\left(2/\zeta_h\hat{Y}^2\right)^{1/3}$
Amplitude of transmissibility at high frequencies $\left\|T_F\right\|_{\Omega\gg1}$ **or** $\left\|T_D\right\|_{\Omega\gg1}$	$2\zeta/\Omega$	$1/\Omega^2$	$2\zeta/\Omega$	$\zeta_h\hat{Y}^2/2\Omega$
Frequency at which the damping force starts to dominates Ω_d	$1/2\zeta$	∞	$1/2\zeta$	$2/\zeta_h\hat{Y}^2$
Minimum force or base displacement	-	$4\sqrt{(\zeta^3/\zeta_h)}$	-	$4\sqrt{(\zeta^3/\zeta_h)}$
Maximum force or base displacement	-	$\zeta_h/250$	-	$\zeta_h/250$
Ratio of maximum to minimum force or base displacement	-	$\left(\frac{\zeta_h}{\zeta}\right)^{3/2}\times10^{-3}$	-	$\left(\frac{\zeta_h}{\zeta}\right)^{3/2}\times10^{-3}$
Isolation frequency Ω_I	$\sqrt{2}$	$\sqrt{2}$	$\sqrt{2}$	$\sqrt{2}$

Source: Adapted from Bing Tang and Brennan (2013) manipulating the subsequent expression, the displacement transmissibility of the nonlinear system at resonance becomes

$$\left|T_{\mathrm{D}}\right|_{\Omega=1} \approx \sqrt[3]{2/\zeta_{\mathrm{h}}\hat{Y}^2} \tag{3.30}$$

For the nonlinear isolator to have a better performance than the linear isolator, the inequality $\left(2/\zeta_{\mathrm{h}}\hat{Y}^2\right)^{1/3} \leq 1/2\zeta$ should be satisfied. This means that the amplitude of the base displacement should be $\hat{Y} \geq 4\sqrt{\left(\zeta^3/\zeta_{\mathrm{h}}\right)}$. As the relative displacement amplitudes have a limiting value of $0.2a$, similar to that for the force-excited system, it leads to the restriction $\hat{Y} \leq \zeta_{\mathrm{h}}/250$ (see Fig. 3.7). The important values from this analysis for the linear and the non-linear isolator are shown in Table 3.1

As $\hat{F}_{\mathrm{e}} \leq \zeta_{\mathrm{h}}/250$ and if $\zeta = 0.1$ and $\zeta_{\mathrm{h}} = 10$ then the maximum allowable value for the excitation force is $\hat{F}_{\mathrm{e}} = 0.4\zeta$, and then the maximum allowable base displacement amplitude for the base excited system is $\hat{Y} = 0.4\zeta$. These are the values used in the plots to try and show the maximum effect.

3.4 Transmissibility for High Amplitude Excitation

When the amplitude of excitation for the nonlinear isolator is such that the relative displacement is higher than $0.2a$ the results from the previous study of Section 3.3 cannot to be applied and then it is necessary to return to the actual form of the equations of motion Eqs (3.3) and (3.5) which can be written in dimensionless form as

$$\hat{x}'' + 2\zeta_{\mathrm{h}}\frac{\hat{x}^2}{1+\hat{x}^2}\hat{x}' + \hat{x} = \hat{F}_{\mathrm{e}}\cos\Omega\tau \tag{3.31}$$

$$\hat{z}'' + 2\zeta_{\mathrm{h}}\frac{\hat{z}^2}{1+\hat{z}^2}\hat{z}' + \hat{z} = \Omega^2\hat{Y}\cos\Omega\tau \tag{3.32}$$

To calculate the force and displacement transmissibility for high excitation amplitudes from Eqs. (3.31) and (3.32) the system is excited at single frequencies. The time responses of the system $\hat{x}$ and $\hat{z}$ are obtained by solving the differential equations by means of the fourth-order Runge-Kutta method at each excitation frequency, employing the *Matlab*® function *Ode45.* The transients are discarded, since the principal interest is on responses at the excitation frequencies and at three times this frequency. From the steady state responses their maximum amplitudes are taken to calculate the forces through the spring and the damper, which correspond to the second and the third terms on the left sides of Eqs. (3.31) and (3.32). They are then summed and divided by the excitation force amplitude, which is known, to obtain the force transmissibility for high amplitude excitation.

A similar equation is obtained for the displacement transmissibility. Once a transmissibility value has been determined for one frequency the process is repeated for the next frequency, with a small increment in frequency, until the whole frequency range is covered.

Force transmissibilities for different values of excitation amplitudes are shown in Fig 3.8. It is possible to see that for high levels of excitation the nonlinear system behaves very well at high frequencies, still as if were undamped, but at frequencies close to resonance the transmissibility is affected badly by the nonlinearity of the damping force, although the transmissibility at the resonance frequency remains smaller than for the linear system. Tang and Brennan (2013) have shown that the nonlinear damping force distorts the time histories of the force transmissibility resulting in a response which contains higher order harmonic terms, and that this effect is proportional to the excitation amplitude. In the next chapter this effect is studied in detail.

In Fig. 3.9 the displacement transmissibility of the nonlinear isolator for different values of high amplitudes of excitation is shown. It is possible to see that at resonance and close to it, the system performs even better than for low excitation levels but at high frequencies the displacement transmissibility of the system increases and for some values of excitation this effect is worse than for the linear

Figure 3.8 – Force transmissibility for the nonlinear isolator system with $\zeta = 0.1$ and $\zeta_h = 10$. For: solid line - linear isolator, dashed line - $\hat{F}_e = 0.1$, dashed dotted line - $\hat{F}_e = 0.2$, dotted line - $\hat{F}_e = 0.3$ and dashed line - $\hat{F}_e = 0.5$ (dB value ref. unity).

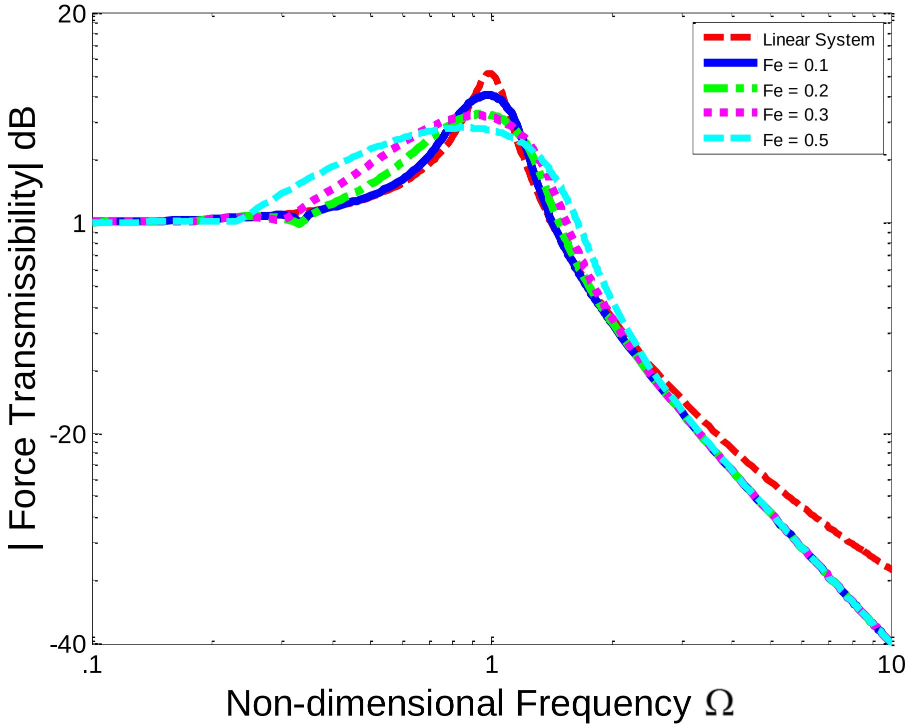

Source: Elaborated by the author

system. This is due to the relation between the frequency at which the damping force starts to dominate the transmissibility and the excitation amplitude, established in the last section ($\Omega_d = 2/\zeta_h \hat{Y}^2$).

Directly from Fig 3.9 can be seen that depending on the situation, the transmissibility at high frequencies can be reduced be reducing ζ_h and accepting some detrimental effect at resonance. As Tang and Brennan (2013) mention, this also occurs with the linear system, as there is a trade-off between reducing the response at resonance and increasing the transmissibility at higher frequencies.

Figure 3.9 – Displacement transmissibility for the nonlinear isolator system when $\zeta = 0.1$ and $\zeta_h = 10$. For: solid line - linear isolator, dashed line - $\hat{Y}_e = 0.1$, dashed dotted line - $\hat{Y}_e = 0.2$, dotted line - $\hat{Y}_e = 0.3$ and dashed line $\hat{Y}_e = 0.5$ (dB value ref. unity).

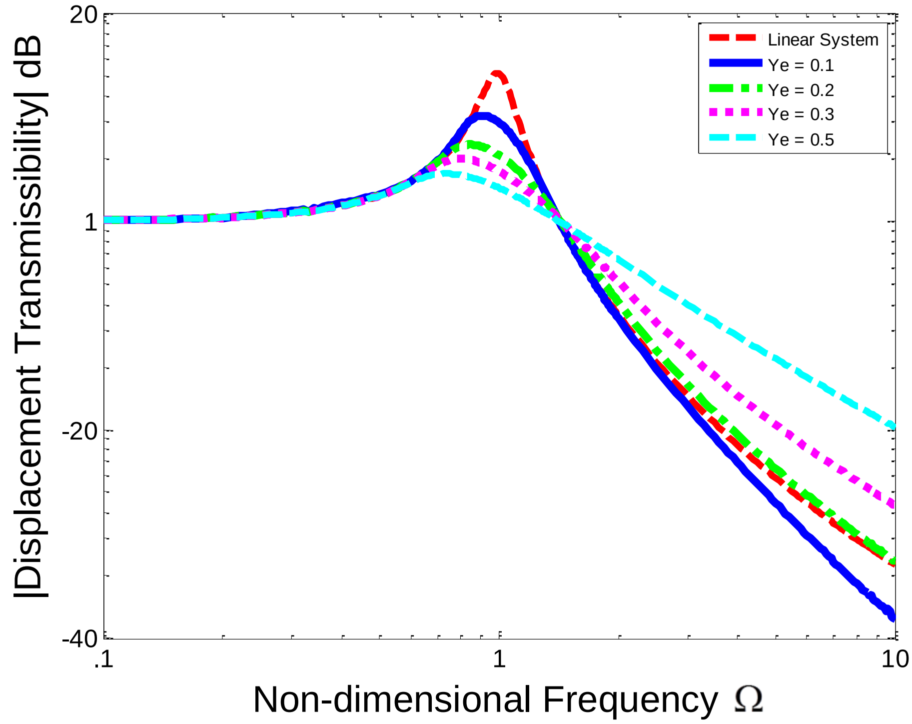

Source: Elaborated by the author

3.5 Conclusions

In this chapter it has been shown that the nonlinear damping force produced by a horizontal damper which is perpendicular to the spring force and to the movement direction in an isolator, can be approximated by an equivalent linear viscous damping force, for low displacement amplitudes, without there being a considerable difference in the energy dissipated. Also, this nonlinear damping force is proportional to the square of the relative displacement amplitude between the mass and the base. This is beneficial for a vibration isolator as the damping force is large when the amplitude is large and small when the amplitude is small.

When the system is excited with *low amplitudes* it was found that at the resonance frequency its force and displacement transmissibilities are lower than for the linear isolator and therefore the nonlinear system performs better than the linear system, but there are conditions on the minimum amplitudes of force and displacement excitation below which the nonlinear system will perform worse than the linear system (see Table 3.1). At frequencies when $\Omega \gg 1$ it was shown that with respect to the force transmissibility, the nonlinear isolator performs better than the linear isolator as the force transmitted through the damper is negligible compared with the force transmitted to the spring and the system behaves as if it were undamped. Concerning the displacement transmissibility of the nonlinear system it was found that it perform betters than the linear system but there is a detrimental effect as it depends on $1/\Omega$ (see Table 3.1).

When the system is excited with a *high amplitude* it was shown that for the force transmissibility the nonlinear isolator at resonance performs better than the linear system, but close to the resonance there is an unfavourable effect which increases the transmissibility at these frequencies. It also was shown that at frequencies when $\Omega \gg 1$ the force transmissibility of the nonlinear system is very good since the system behaves as if it were undamped. Concerning the displacement transmissibility, at resonance the nonlinear isolator performs better than the linear isolator, but the frequency at which the damper begins to dominate the transmissibility decreases with the excitation amplitude. At high excitation amplitude this results in a detrimental effect on the displacement transmissibility.

4 DETAILED ANALYSIS OF THE NONLINEAR ISOLATION SYSTEM

4.1 Introduction

In the previous chapter it was shown that the force transmissibility of the nonlinear damping system has desirable characteristics at high frequencies. However at frequencies close to the resonance frequency, the system has undesirable characteristics, even though the peak at resonance is smaller than that of the linear system (see Fig. 3.8). In this chapter an investigation is carried out into the causes of these adverse effects. The time histories of the internal forces are decomposed into their spectral components using the *Fourier series* in the resonance region, and these are studied to determine the sources of the nonlinearities and the way in which they propagate through the system.

4.2 Brief Review of the Fourier series

The time histories for the transmitted forces and its components are periodic which repeats every period of the excitation frequency $T = 2\pi / \Omega$, where Ω is the excitation frequency, see for instance Fig. 4.1. Periodic signals can be analysed using the Fourier series. A periodic signal can be represented by adding together sine and cosine functions of appropriated frequencies, amplitudes and relative phases (SHIN; HAMMOND, 2008, p 31).

The *Fourier series* representation of a periodic signal is given by (Shin and Hammond, 2008, p 312)

$$x(t) = \frac{a_0}{2} + \sum_{n=1}^{\infty}\left[a_n \cos\left(\frac{2\pi nt}{T}\right) + b_n \sin\left(\frac{2\pi nt}{T}\right)\right] \qquad (4.1)$$

where $n = 1, 2, 3, 4, \ldots$ and the fundamental frequency, which corresponds here to the excitation frequency is $\Omega = 2\pi / T$, and the higher frequencies are integers multiples of this. The amplitudes of the higher frequencies than the fundamental are called *harmonics*. The quantity $a_0 / 2$ is the mean value of the signal and the coefficients a_n and b_n are the Fourier coefficients which are used to calculate the amplitude and the phase of each harmonic as follows:

$$\begin{aligned} A_n &= \sqrt{a_n^2 + b_n^2} \\ \phi_n &= \tan^{-1}\left(-b_n / a_n\right) \end{aligned} \tag{4.2}$$

where A_n is the amplitude of the nth harmonic and ϕ_n its phase angle. The Fourier series representation in terms of the amplitudes and the phase is given by

$$x(t) = \frac{a_0}{2} + \sum_{n=1}^{\infty} A_n \cos\left(2\pi n\Omega + \phi_n\right) \tag{4.3}$$

The Fourier coefficients are calculated from (Shin and Hammond, 2008, p 32)

$$\begin{aligned} \frac{a_0}{2} &= \frac{1}{T}\int_0^T x(t)dt \\ a_n &= \frac{2}{T}\int_0^T x(t)\cos\left(\frac{2\pi nt}{T}\right)dt \qquad n = 1, 2, 3,... \\ b_n &= \frac{2}{T}\int_0^T x(t)\sin\left(\frac{2\pi nt}{T}\right)dt \end{aligned} \tag{4.4}$$

The amplitudes and the frequencies are used to create the spectrum of the signal to determine the influence of each harmonic in the original signal. Depending on the signal it can be composed by odd or even harmonics or a combination of the two.

4.3 Study of the harmonic content of the signals

In this section the Fourier series is used to analyse the transmitted force in the resonance region as there is undesirable behaviour in this region, see Fig. 3.8. The resonance region is roughly the frequency $0.3 < \Omega < 1.6$ so the present study will focus on the transmitted force at these frequencies. Taking in account the fact that the damping force is the cause of the nonlinearity of the system, as shown in Eq. (3.31), it is thought that this is the cause of the adverse behaviour. Tang and Brennan (2013) made the following comment:

> *The nonlinear damping force has a profound effect on the transmissibility response and the time history response at the excitation frequency. The nonlinear damping force distorts the time history curves of the force transmissibility with the undesirable result that there are many high order harmonic terms in the response. The larger the excitation force amplitude, the stronger the influence on the force transmissibility curves* (Tang and Brennan, 2013, p. 517).

Following this indication the time history for the transmitted force as well as its frequency spectrum at different excitation frequencies in the resonance region are analysed. As the transmitted force is composed of the force transmitted by the spring and the force transmitted by the damper, the time histories of those forces with their frequency spectra are compared and analysed to determine the influence of each one of this forces on the transmitted force. Using the definition of the damping force from Eq. (3.31) and setting $z = x$, the damping force is decomposed into the velocity of the mass $\hat{x}'$ and the *damping coefficient* c_{f} which has the form

$$c_{\mathrm{f}} = 2\zeta_h \left(\frac{\hat{x}^2}{1+\hat{x}^2} \right) \tag{4.5}$$

Hence the damping force can be written as $f_{\mathrm{d}} = c_{\mathrm{f}}\hat{x}'$. The time history of the damping coefficient and the velocity as well as its frequency spectra are also analysed with the aim to determine the influence of each of them on the nonlinearity of the damping force. This procedure is conducted for the nonlinear system when excited at five different frequencies; the first four of them are in the resonance region: $\Omega = 0.3$, $\Omega = 0.5$, $\Omega = 1$, $\Omega = 1.5$, while the last one belongs to the beginning of the isolation region: $\Omega = 2$.

4.3.1 Spectrum of the Transmitted Force

From Eq. (3.31) can be obtained the expression for the non-dimensional transmitted force $\hat{f}_t(t) = 2\zeta_h \frac{\hat{x}^2}{1+\hat{x}^2}\hat{x}' + \hat{x}$, Composed by the force transmitted through the damper and the force transmitted through the spring, respectively. The non-transmitted force is composed of non-dimensional expression; therefore *in this section the transmitted forces through the spring and the damper, as well as the total transmitted force are all non-dimensional forces. Also the velocity and the nonlinear damping coefficient are non-dimensional variables*.

To demonstrate the effect of the external excitation on the nonlinear system, the maximum value of the force in Chapter 3 is used, i.e., $\hat{F}_e = 0.5$, and the horizontal damping coefficient $\zeta_h = 10$.

Figure 4.1 shows the time histories for the force transmitted through the nonlinear isolation system for the excitation frequencies $\Omega = 0.3$, $\Omega = 0.5$, $\Omega = 1$, $\Omega = 1.5$ and $\Omega = 2$, together with their respective frequency spectra. Figs. 4.1 (a) and (b) show the time history for the transmitted force at $\Omega = 0.3$ and its frequency spectrum respectively; the harmonics shown in Fig. 4.1 (b) with the mean value (DC value) at zero frequency are used to reconstruct the original transmitted force curve in Fig 4.1 (a) by means of the Fourier series. This reconstruction, which serves to validate the frequency spectrum, is overlaid on the original curve. In Fig 4.1 (a) the first harmonic is also plotted which represents the transmitted force at the excitation frequency and which closely follows the transmissibility curve, and the excitation force, which has an amplitude $\hat{F}_e = 0.5$.

There can be seen that at this low frequency the maximum value of the transmitted force reaches nearly three times the amplitude of the excitation force, the presence of higher order harmonics can also be seen, which makes the transmitted force larger than the amplitude of first harmonic. Figure 4.1 (b) reveals that it only odd harmonics are needed to reconstruct the transmitted force curve and that the most important influence in the transmissibility is the force transmitted at the excitation

Figure 4.1 - Time history for the non-dimensional transmitted force through the nonlinear isolation system and its frequency spectrum when $\zeta_h = 10$ and $\hat{F}_e = 0.5$ for a) $\Omega = 0.3$, c) $\Omega = 0.5$, e) $\Omega = 1$, g) $\Omega = 1.5$, i) $\Omega = 2$. Blue solid line – time history for the transmitted force, yellow dotted line – Fourier series of the time history, red dashed line – first harmonic of the Fourier series, black solid line – excitation force, magenta horizontal line – mean value (DC level) of the signal. b), d), f) h) and j) – Frequency spectrum with the DC value at zero and the first fifteen harmonics from the Fourier series of the time history for the transmitted force curves shown in a), c), e), g), and j).

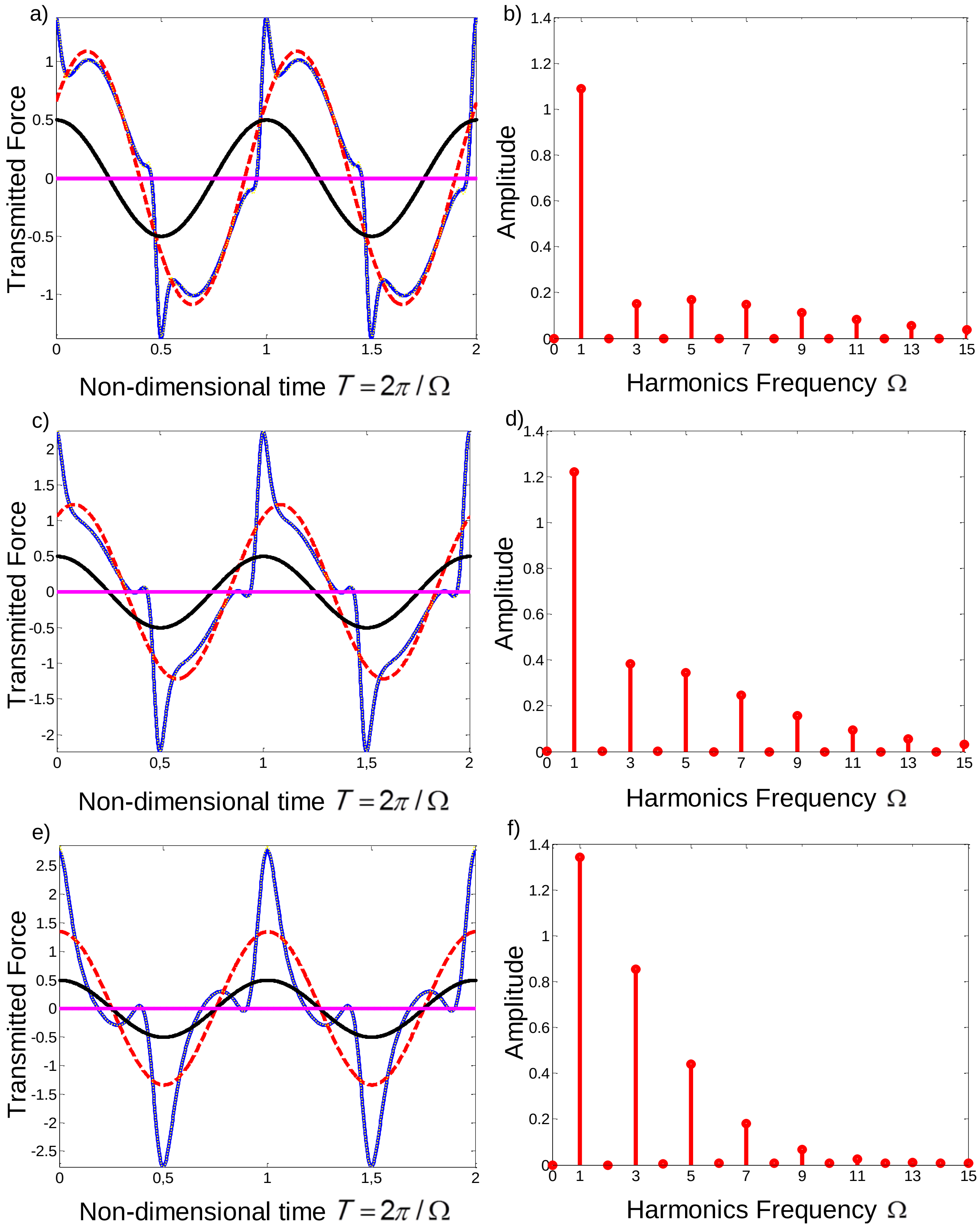

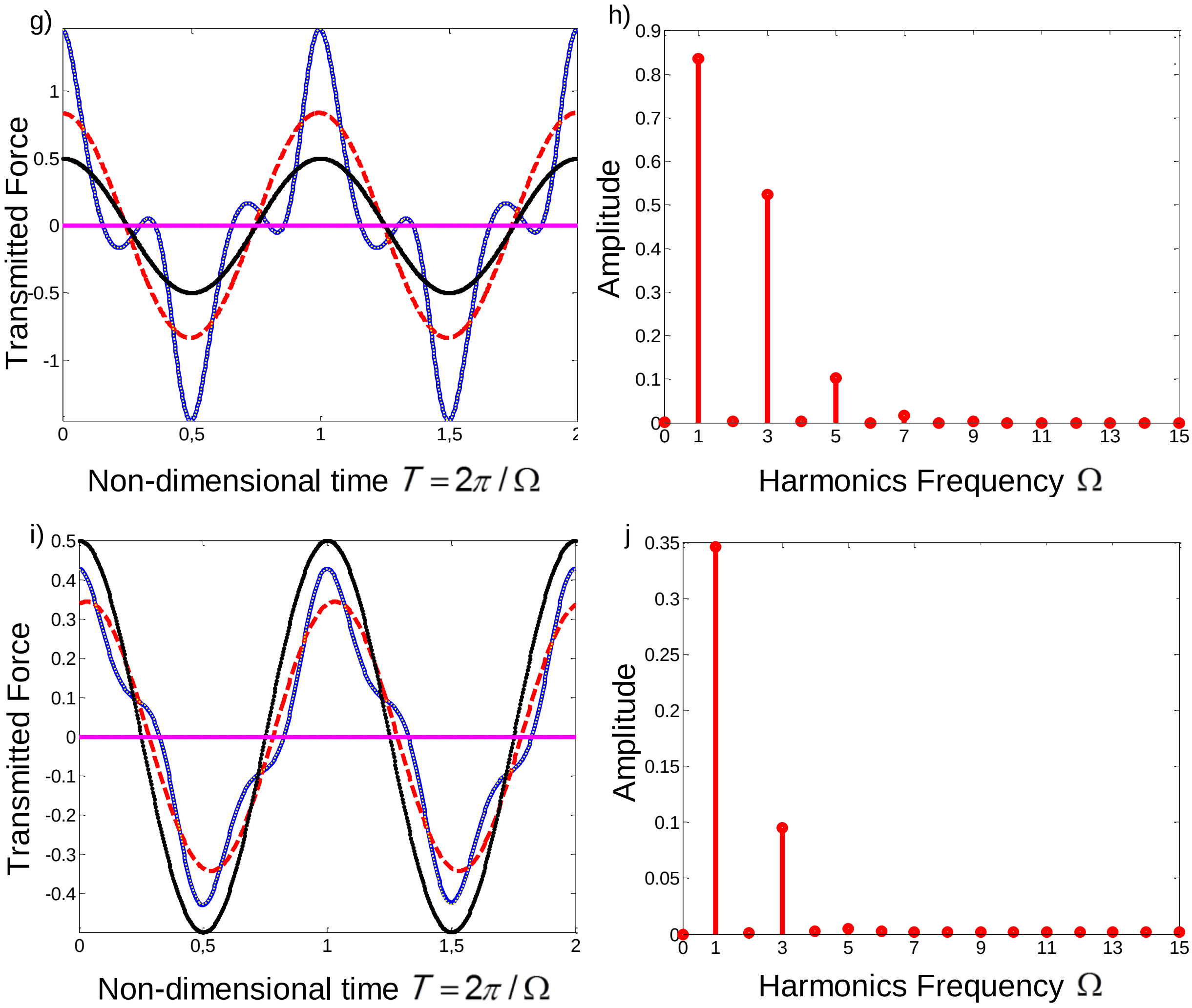

Source: Elaborated by the author

frequency (1st harmonic). Its amplitude is nearly 80% of the maximum value of the transmitted force curve. The force transmitted at the excitation frequency is more than twice the amplitude of the excitation force; the influence of the force at three, five, seven and nine times the excitation frequency is not so large but does adversely affect the transmitted force. Harmonics higher than the 9th have a negligible influence on the transmissibility.

When the system is excited with a frequency $\Omega = 0.5$, (see Figs 4.1 (c) and (d)), the transmitted force increases considerably being nearly five times the amplitude of the excitation frequency; the influence of the force transmitted at the excitation frequency continues to be significant since is nearly half of the total transmitted force is transmitted by the first harmonic. Comparing Fig. 4.1 (b) and (d) can be seen that the amplitude of the first harmonic is almost the same as for $\Omega = 0.3$ unlike the amplitudes of the 3rd, 5th, 7th and 9th harmonics which are larger for $\Omega = 0.5$ than for $\Omega = 0.3$.

When the system is excited at resonance $\Omega = 1$, which is illustrated in Figs. 4.1 (e) and (f), the transmitted force increases just a little compared with the excitation force at $\Omega = 0.5$, its maximum value is five times greater than the amplitude of the excitation force. The transmitted force at the excitation frequency is still nearly half of the total transmitted force. Unlike the frequency spectrum of the transmitted force at $\Omega = 0.5$ Fig. 4.1 (f) shows a significant contribution of the transmitted force mainly at three times and five times the excitation frequency and to a lesser extent at seven times the excitation frequency. The influence of harmonics higher than the 7th can be neglected. The time history of the transmitted force at the resonance has a slightly different shape than at lower frequencies, having its maximum and minimum values greater than the maximum and minimum of the 1st harmonic and the excitation force. At $\Omega = 1.5$ the transmitted force decreases, again its maximum value is nearly three times the amplitude of the excitation force. This is illustrated in Figs. 4.1 (g) and (h), where it can be seen that the transmitted force is mainly composed of the 1st and the 3rd harmonic, and to some extent, the 5th harmonic. There is no influence of harmonics higher than the 5th in the time history of the transmitted force.

In the isolation region at $\Omega = 2$ the force transmitted is, as expected, less than the amplitude of the excitation force and is composed of the 1st and the 3rd harmonic, see Figs. 4.1 (g) and (h). There is no influence of harmonics higher than the 3rd. The amplitude of the first harmonic is nearly 70% of the amplitude of the transmitted force. The transmitted force at this excitation frequency starts to be similar to a sine wave.

4.3.2 Force Through the Spring

As mentioned previously the total transmitted force to the base consists of the force transmitted through the spring and the force transmitted through the damper. In order to establish what is the importance of each component on the transmitted force in this subsection, the time history for the force transmitted through the spring and its frequency spectrum are studied. As in the previous section the frequencies $\Omega = 0.3$,

Figure 4.2 - Time histories for the non-dimensional force through the spring of the nonlinear isolation system and its frequency spectrum when $\zeta_h = 10$ and $\hat{F}_e = 0.5$ for a) $\Omega = 0.3$, c) $\Omega = 0.5$, e) $\Omega = 1$, g) $\Omega = 1.5$, i) $\Omega = 2$. Blue solid line – time history for the force through the spring, yellow dotted line – Fourier series of the time history, red dashed line – first harmonic of the Fourier series, black solid line – excitation force, magenta horizontal line – mean value (DC level) of the signal. b), d), f), h) and j) – Frequency spectrum with the DC value at zero and the first fifteen harmonics from the Fourier series of the time history for the force through the spring curves shown in a), c), e), g) and j).

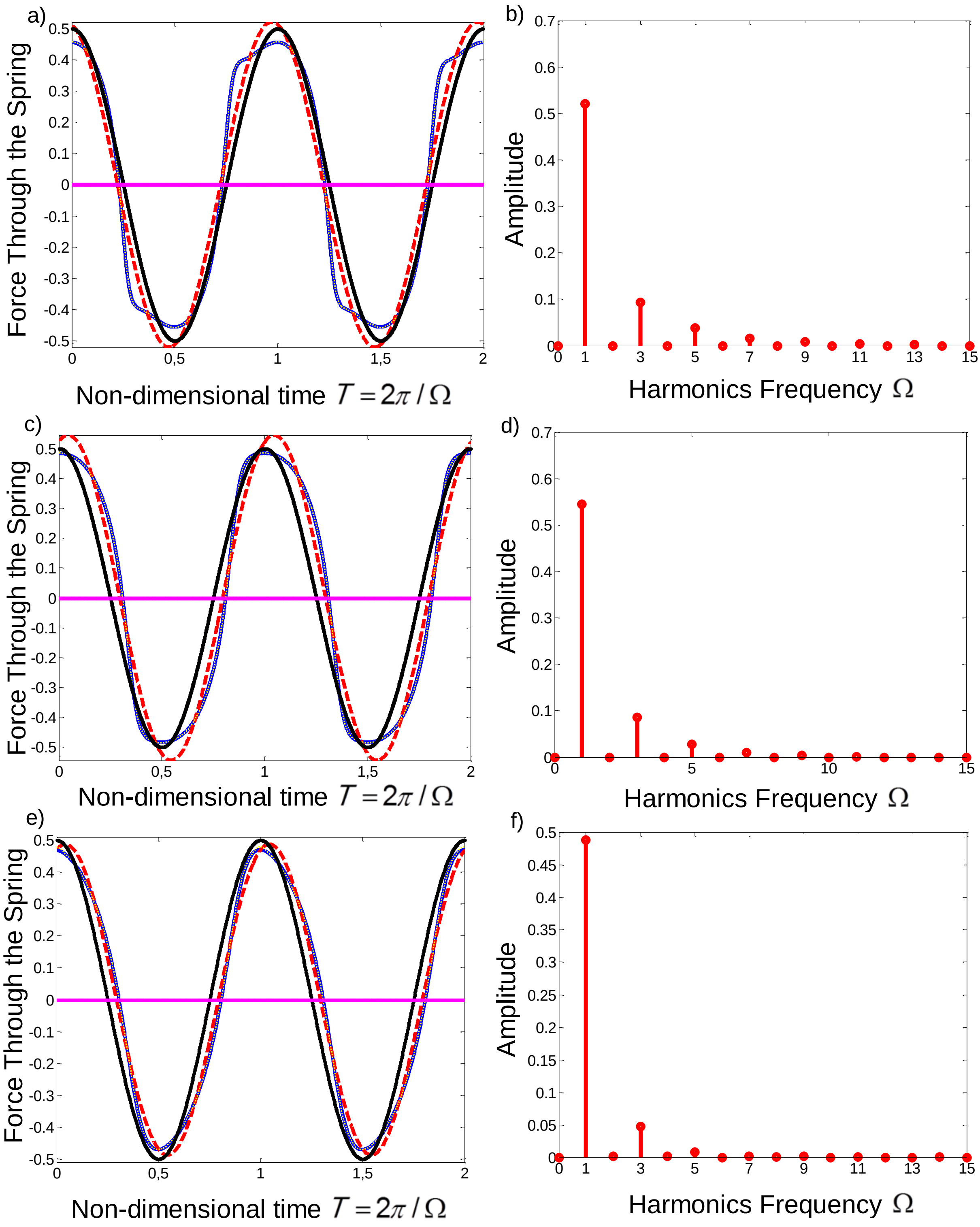

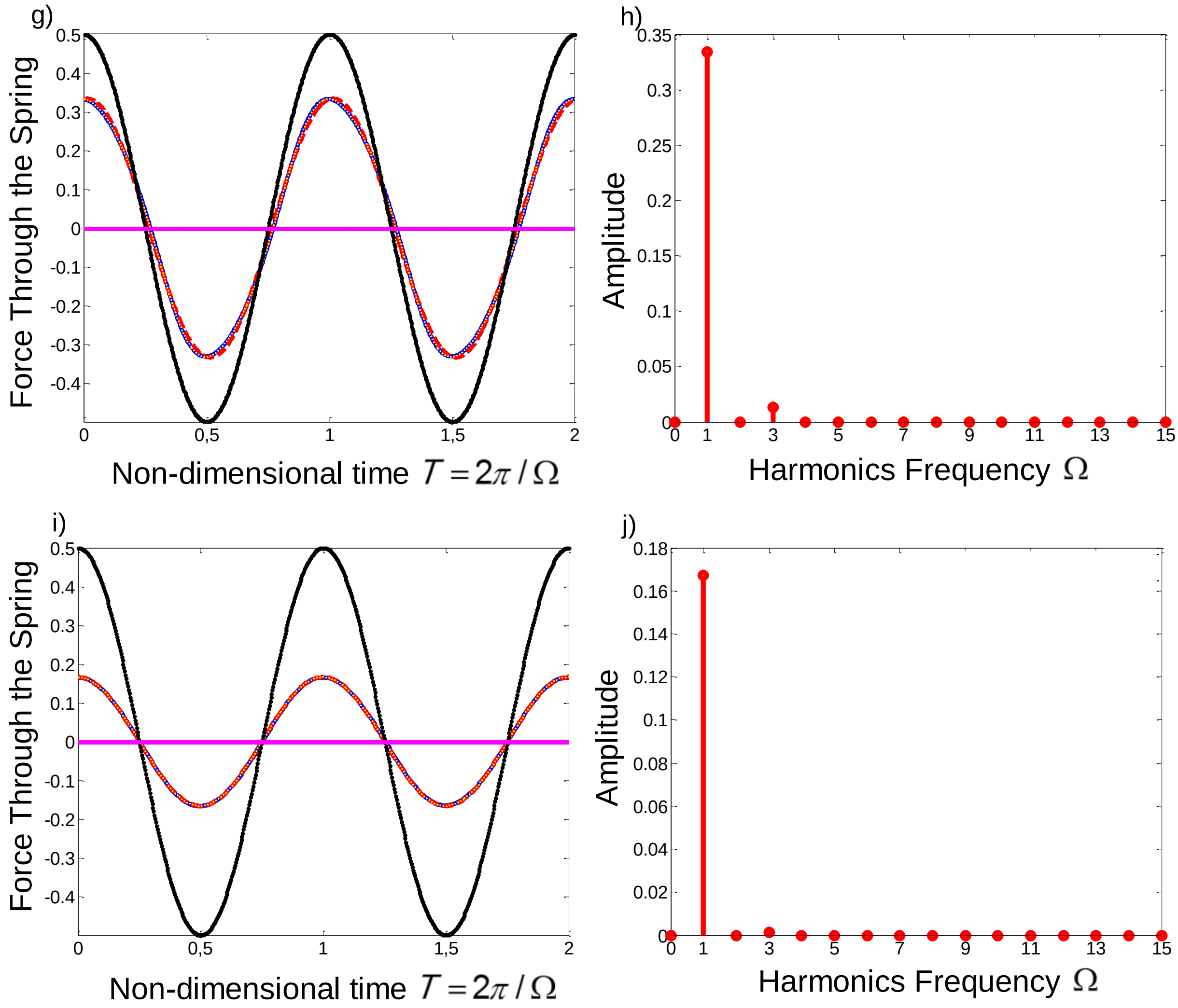

Source: Elaborated by the author

$\Omega = 0.5$, $\Omega = 1$, $\Omega = 1.5$ and $\Omega = 2$ are considered. There is another important point to be made. The non-dimensional force through the spring corresponds to the third term in the left side of Eq. (3.31). It is equal to the non-dimensional displacement, so the force through the spring and the displacement of the mass have the same behaviour.

Figure 4.2 shows the time histories for the force transmitted through the spring together with their respective frequency spectra at five different frequencies; four of which are in the resonance region and the other one corresponds to the beginning of the isolation region. Figures 4.2 (a) and (b) shows the force transmitted through the spring when the system is excited at $\Omega = 0.3$ and its frequency spectrum, it can be seen that the amplitude of the force is a little smaller than the amplitude of the excitation force and is mainly composed of the 1st and to a lesser degree the 3rd harmonic. This feature maintains when the system is excited at $\Omega = 0.5$ (see Figs. 4.2 (c) and (d)) and $\Omega = 1$ (Figures. 4.2 (e) and (f)), in which the amplitude of the force through the spring is smaller but almost equal to the amplitude of the excitation force. The time histories are slightly distorted mainly by the small influence of the 3rd harmonic and the negligible 5th harmonic. They are very similar to the sine wave representing the excitation force. Thus at frequencies less than or equal to the resonance frequency, the force transmitted through the spring is almost equal to the amplitude of the excitation force. It also can be seen that the displacement of the mass is only slightly distorted when the system is excited at frequencies below the resonance frequency.

Figures. 4.2 (g) and (h) shows the transmitted force through the spring at $\Omega = 1.5$ and its frequency spectrum. It can be seen that the amplitude of the force transmitted through the spring decreases, it is nearly 70% of the amplitude of the excitation force and is basically composed of the 1st harmonic. When the system is excited at $\Omega = 2$, the amplitude of the force transmitted through the spring is nearly 30% the amplitude of the excitation force. This is illustrated in Figs 4.2 (i) and (j). So at frequencies higher than the resonance frequency the transmitted force becomes sinusoidal and the force transmitted through the spring decreases.

4.3.3 Force through the Damper

Figure 4.3 shows the time history for the force through the damper and its frequency spectrum for $\Omega = 0.3$, $\Omega = 0.5$, $\Omega = 1$, $\Omega = 1.5$ and $\Omega = 2$. Also shown is the time history of the first harmonic, the excitation force and the mean value. Again, it can be seen that only odd harmonics are needed to reconstruct the original curve. Figures. 4.3 (a) and (b) shows the time history and the frequency spectrum of the force through the damper at $\Omega = 0.3$; it can be seen that the peak value of the transmitted force is less than the amplitude of the excitation force being nearly 80% of this amplitude. Figure 4.3 (b) displays an interesting frequency spectrum. The force transmitted at the excitation frequency is nearly half the amplitude of the excitation force but unlike almost all the previous frequency spectra, the harmonics higher than the fundamental frequency do not decrease as the frequency increases. The 3rd harmonic is very small and the 5th, 7th, 9th, 11th 13th have a considerable amplitude and it is mainly these that compose the other part of the transmitted force.

Figure 4.3 - Time histories for the non-dimensional force through the damper of the nonlinear isolation system and its frequency spectrum when $\zeta_h = 10$ and $\hat{F}_e = 0.5$ for a) $\Omega = 0.3$, c) $\Omega = 0.5$, e) $\Omega = 1$, g) $\Omega = 1.5$, i) $\Omega = 2$. Blue solid line – time history for force through the damper, yellow dotted line – Fourier series of the time history, red dashed line – first harmonic of the Fourier series, black solid line – excitation force, magenta horizontal line – mean value (DC level) of the signal. b), d), f), h) and j) – Frequency spectrum with the DC value at zero and the first fifteen harmonics from the Fourier series of the time history for the force through the damper curves shown in a), c), e), g) and j).

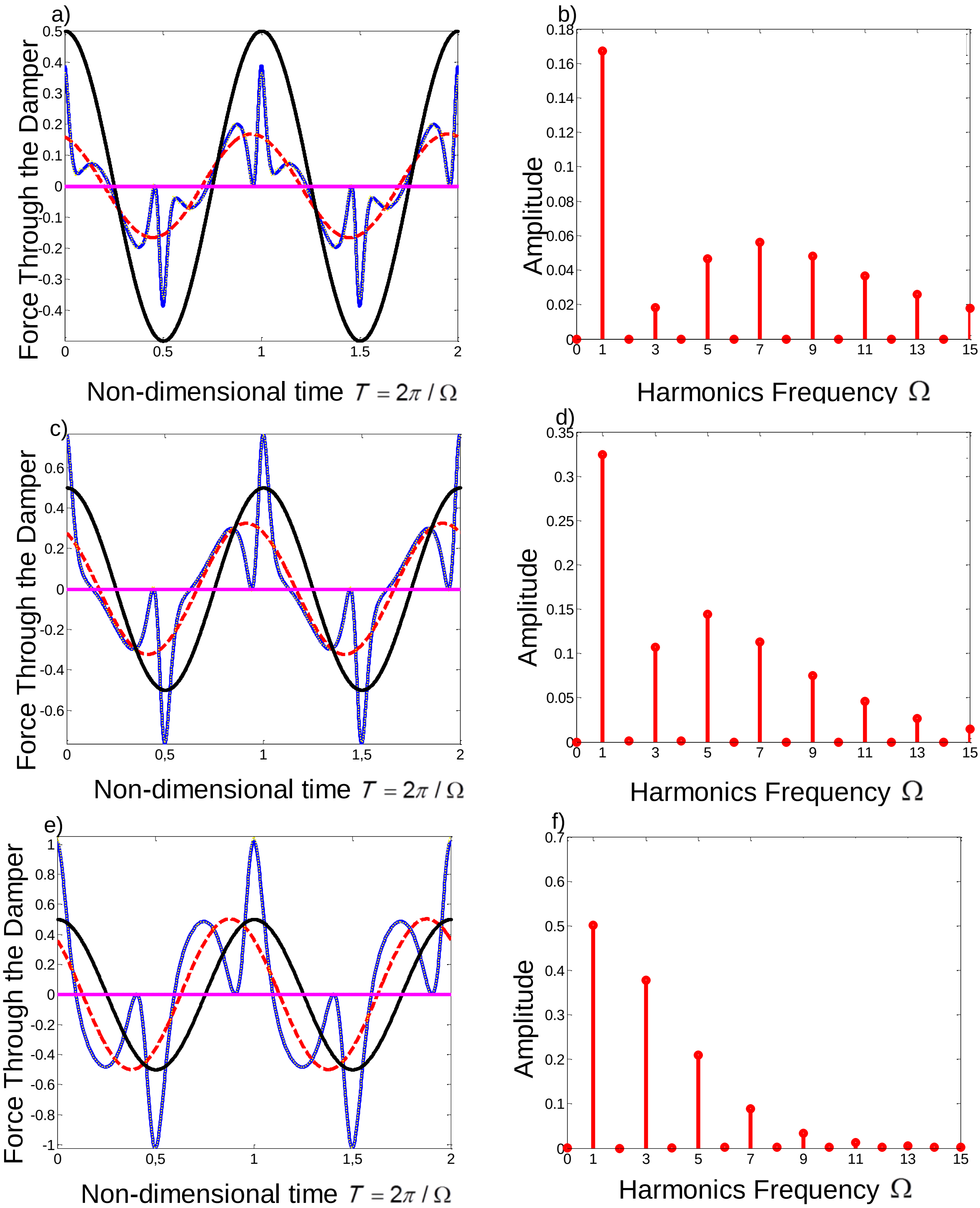

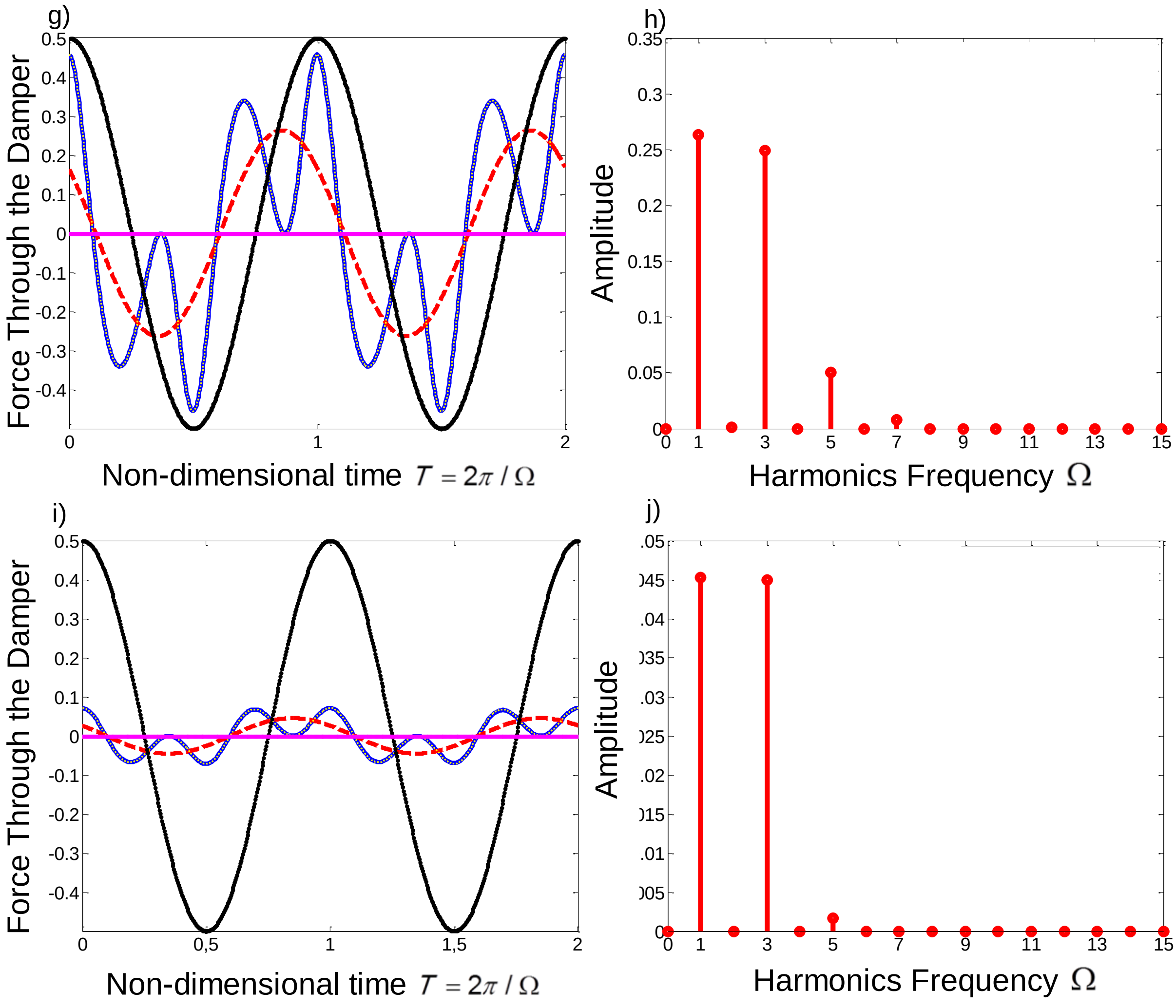

Source: Elaborated by the author

This creates the distortion in the force transmitted through the damper curve as shown in Fig. 4.3 (a). It also causes the distortion in the time history of the transmitted force.

At frequency $\Omega = 0.5$ the transmitted force through the damper broadly maintains its sinusoidal shape but increases its maximum value. It is nearly 20% larger than the excitation force. The force transmitted at the excitation frequency is again nearly half of the total transmitted force through the damper and this is true for every time history shown in Fig 4.3. However, the influence of the 3rd harmonic becomes relevant while the influence of the 13th becomes negligible. At the resonance frequency $\Omega = 1$ the force transmitted through the damper increases, it is nearly twice the excitation force, see Fig. 4.3 (e) and (f). The shape distorts more, but maintains a similarity with Fig. 4.3 (c). The force transmitted through the damper is mainly composed of the 1st, the 3rd, the 5th, and the 7th harmonic, and the rest of the harmonics are negligible.

At $\Omega = 1.5$ the force transmitted through the damper is just a little smaller than the amplitude of the excitation force, see Fig 4.3 (g). From Fig 4.3 (h) can be seen that the force through the damper is mainly composed if the 1st and the 3rd harmonic and in lesser extend of the 5th harmonic.

In the isolation region at $\Omega = 2$ the force transmitted through the damper reduces considerably, see Figs 4.3 (i) and (j). It is nearly 15% of the amplitude of the excitation force and consists of the fundamental and the 3rd harmonic. Comparing the force transmitted through the spring (Figs 4.2 (i)) and the force transmitted through the damper (Figs 4.3 (i)) at this frequency it can be seen that the force through the damper is nearly one quarter of the force transmitted through the spring. This is consistent with the findings in Chapter 3 where it was found that at this frequency the transmitted force is mainly dominated by the force trough the spring.

Comparing Figs. 4.2 and 4.3 it can be seen that specifically for the large value use here to the amplitude of the excitation force, the force transmitted through the damper exceeds the amplitude of the excitation force, while the force transmitted through the spring do not do it, whatever the excitation frequency. This is because the large amplitude of the excitation force produces large mass displacements and it makes considerably increase the force through the damper while the force through the spring increases but in a lesser extent. It also can be seen that the distortion in the time history curves of the transmitted force of Fig. 4.1 are due to the force transmitted through the damper, as would be expected, and not to the force through the spring.

4.3.4 Nonlinear Damping Coefficient

The expression of the viscous damping force is the multiplication of two parameters: the damping coefficient which is constant for a linear damper and the relative velocity. For the damper considered in this work the damping coefficient is a

Figure 4.4 - Time histories for the non-dimensional damping coefficient function c_f of the nonlinear damper and its frequency spectrum when $\zeta_h = 10$ and $\hat{F}_e = 0.5$ for a) $\Omega = 0.3$, c) $\Omega = 0.5$, e) $\Omega = 1$, g) $\Omega = 1.5$, i) $\Omega = 2$. Blue solid line – time history the nonlinear damping coefficient c_f, yellow dotted line – Fourier series of the time history, red dashed line – second harmonic of the Fourier series, magenta horizontal line – mean value (DC level) of the signal. b), d), f), h) and j) – Frequency spectrum with the DC value at zero and the first fifteen harmonics from the Fourier series of the time history for nonlinear damping coefficient curves shown in a), c), e), g) and j).

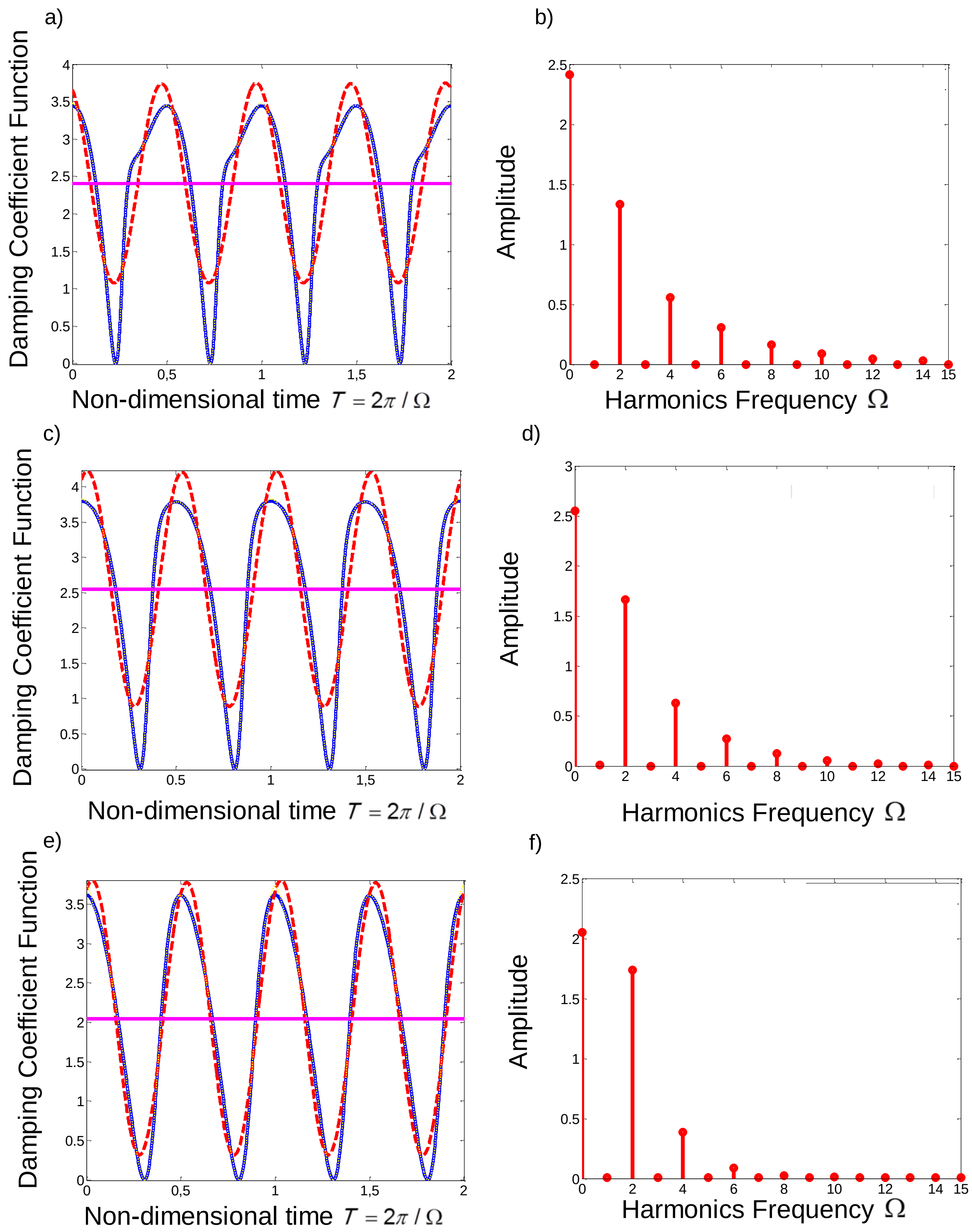

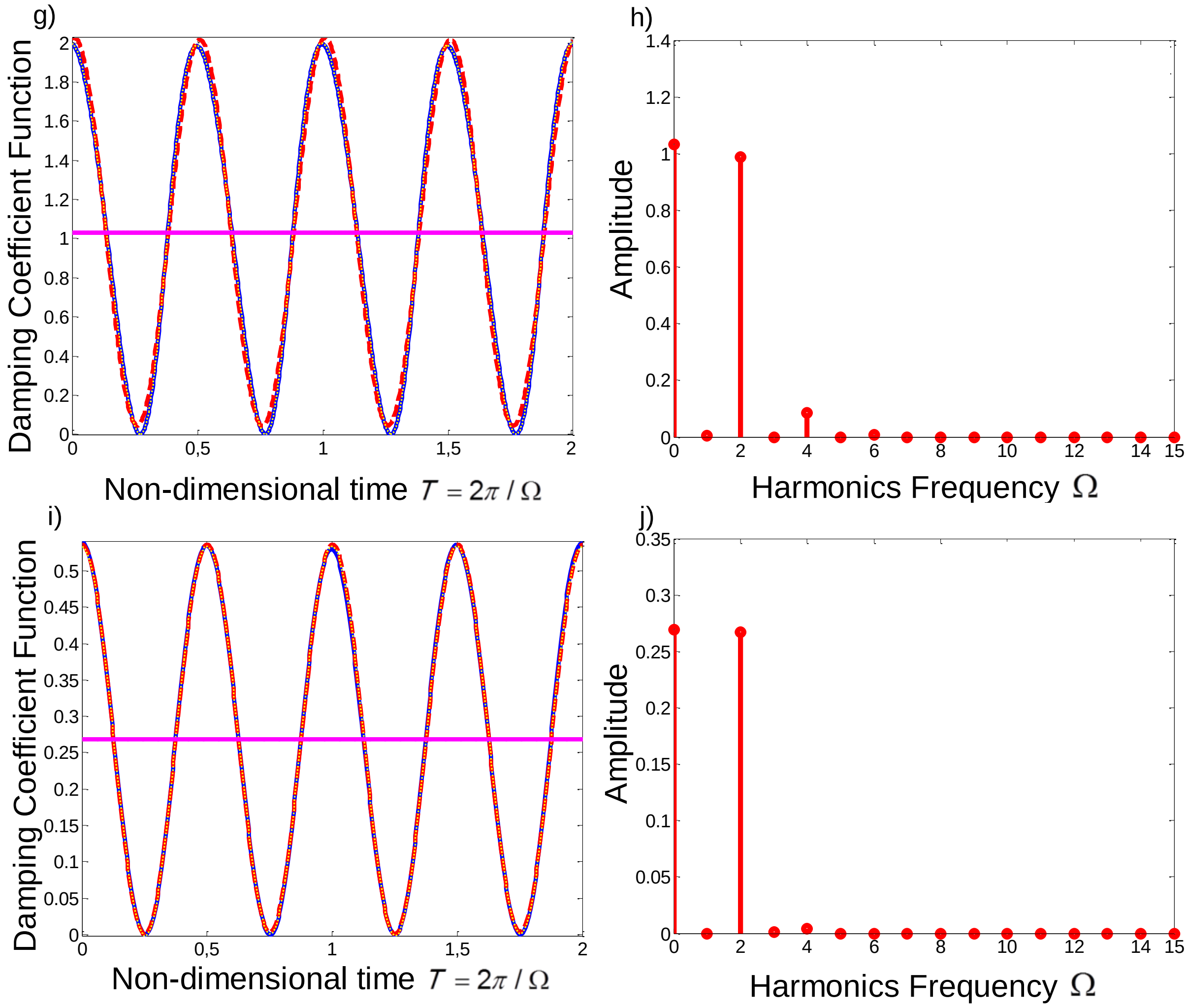

Source: Elaborated by the author

function of displacement and hence time, because of this it is referred as the nonlinear damping coefficient and is denoted by c_f. For the same five excitation frequencies discussed above, the time history and spectrum of c_f are shown in Fig. 4.4.

Examining Eq. (4.5) some insight into the behaviour of c_f can be gained. The first two terms are constant and the term in the parenthesis is the term which governs its nonlinear behaviour. As it depends on the square of the displacement, the damping coefficient curve in time domain would be similar to a sine function squared. This has a mean value and its Fourier series is composed of even harmonics. Its larger values will be at the frequencies in which the displacement has large values (See Fig. 4.1) and the presence of higher harmonics would appear in c_f at the frequencies for which the displacement displays a frequency spectrum with higher harmonics.

The higher displacements for the nonlinear system are at frequencies less than or equal to the resonance frequency, so the higher values for c_f are at the frequencies $\Omega = 0.3$, $\Omega = 0.5$ and $\Omega = 1$. This can be seen in Figs. 4.4 (a), (c) and (e) which show the time histories of c_f for these excitation frequencies. There is a small influence of harmonics higher than the 2^{nd} in the time histories which can be seen clearly in the frequency spectra shown in Figs. 4.4 (b), (d) and (f). Some influence of the 4^{th} harmonic for $\Omega = 1$, and the 4^{th} and the 6^{th} harmonic for $\Omega = 0.5$ and $\Omega = 1$ can be seen. For frequencies higher the resonance frequencies, $\Omega = 1.5$ and $\Omega = 2$ there is a negligible influence of higher harmonics. Only the mean value and the 2^{nd} harmonic are necessary to reconstruct the original signals for the nonlinear damping coefficient, this is shown in Figs. 4.4 (g) and (h) for $\Omega = 1.5$ and Figs. 4.4 (i) and (j) for $\Omega = 2$. At these frequencies the amplitude of c_f starts to reduce, with its amplitude being less than one.

Although the results depend on the parameters used in the beginning of the chapter, which are the same used in Chapter 3, in general it can be concluded that the nonlinear damping coefficient at frequencies inside the resonance region produces the effect of increasing the amplitude of the velocity; as its maximum values are larger than one. On the other hand for frequencies in the isolation region, the nonlinear damping coefficient produces the opposite effect, reducing the amplitude of the velocity; as its maximum values are smaller than one. This is a different effect compared with that of a viscous coefficient damping which is constant whatever the frequency value.

4.3.5 Velocity of the mass

In determining the causes of the unfavourable behaviour of the transmitted force shown in Fig. 3.8, the transmitted force has been decomposed into forces transmitted through the spring and through the damper. The nonlinear force transmitted through the damper can be studied by examining the nonlinear damping coefficient and the velocity of the mass. In this subsection the time history and the

Figure 4.5 - Time histories for the non-dimensional mass velocity of the nonlinear damper and its frequency spectrum when $\zeta_h = 10$ and $\hat{F}_e = 0.5$ for a) $\Omega = 0.3$, c) $\Omega = 0.5$, e) $\Omega = 1$, g) $\Omega = 1.5$, i) $\Omega = 2$. Blue solid line – time history for the mass velocity, yellow dotted line – Fourier series of the time history, red dashed line – first harmonic of the Fourier series, magenta horizontal line – mean value (DC level) of the signal. b), d), f), h) and j) – Frequency spectrum with the DC value at zero and the first fifteen harmonics from the Fourier series of the time history for nonlinear damping coefficient curves shown in a), c), e), g) and j).

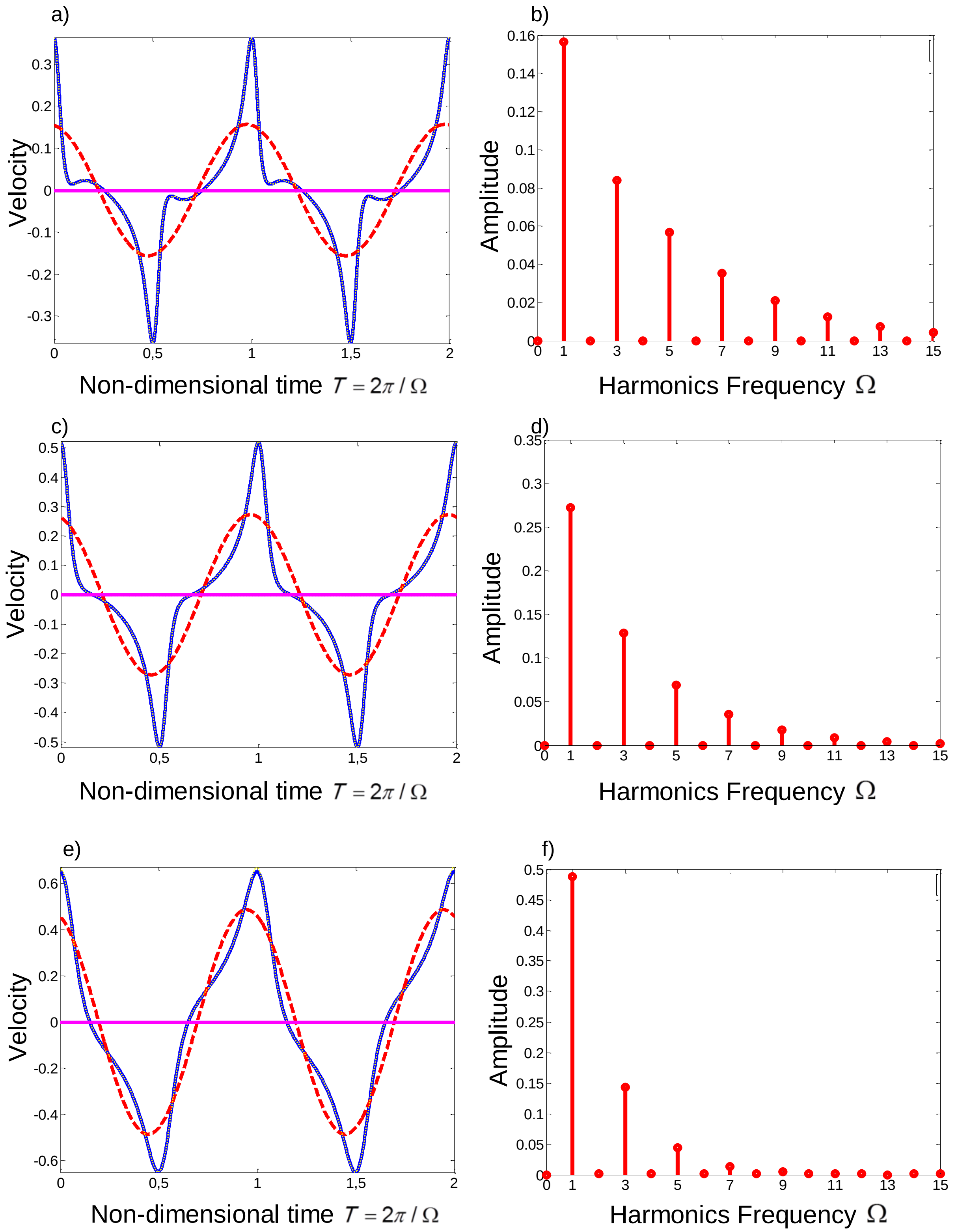

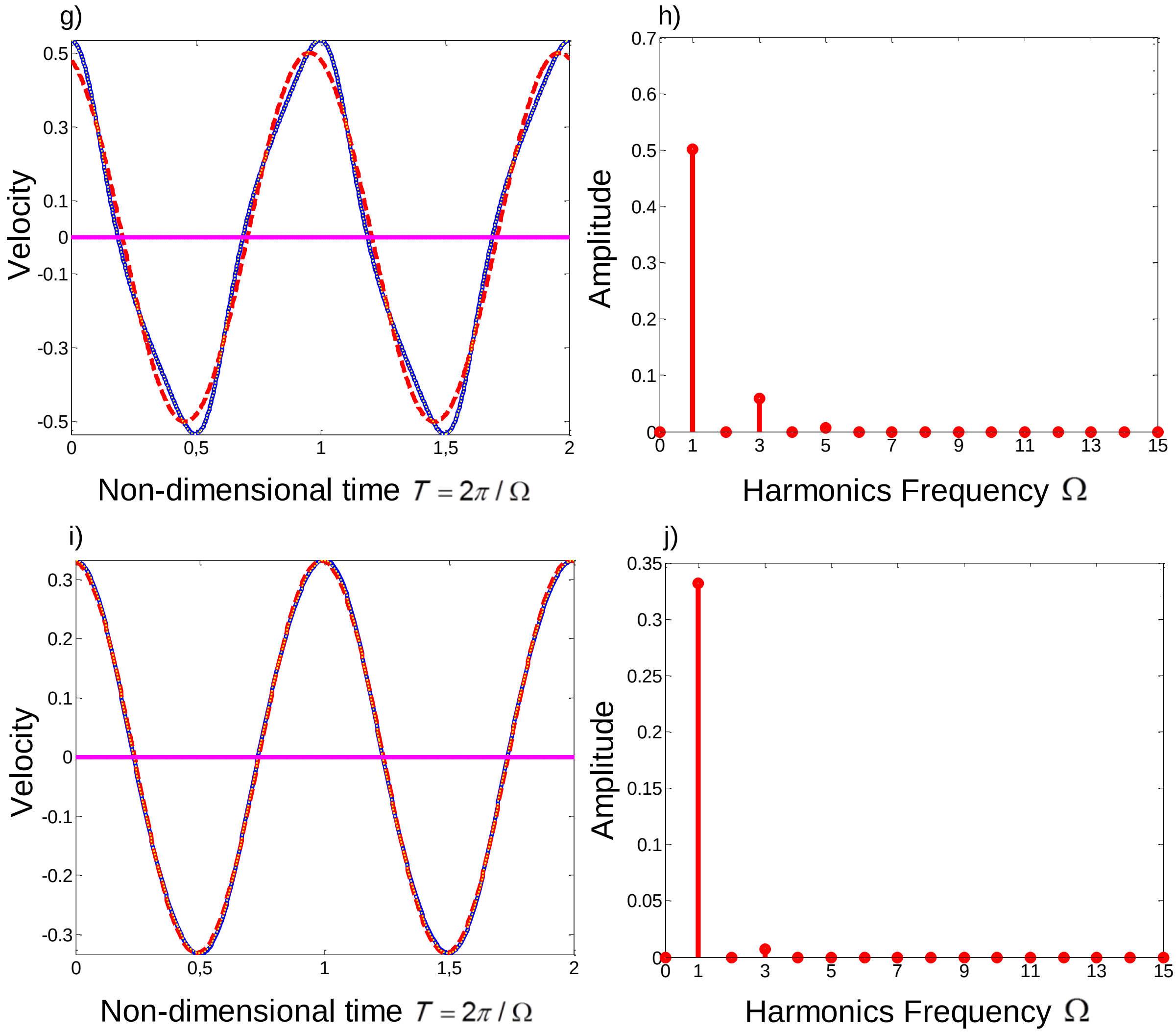

Source: Elaborated by the author

frequency spectra of the velocity of the mass at five excitation frequencies near to the resonance frequency are analysed.

Figure 4.5 shows the time history of the velocity and its frequency spectrum for five different frequencies near to the resonance frequency. Only harmonics are

needed to reconstruct the original curves. At $\Omega = 0.3$ the time history of the velocity is highly distorted (see Fig. 4.5 (a) and (b)), its frequency spectrum reveals that the first harmonic is nearly the 40% of the velocity of the mass and the higher harmonics compose the rest of the velocity. There is an influence of the 3rd, 5th, 7th and 9th harmonics in the reconstruction of the curve and the mean value is zero. At $\Omega = 0.5$ the maximum value of the velocity increases and its time history curve is still considerably distorted. The influence of the higher harmonics is still significant, but only up to the 7th harmonic. Because of this the shape of the curve is very similar to the time history for $\Omega = 0.3$. This is illustrated in Figs. 4.5 (c) and (d).

At the resonance frequency, $\Omega = 1$, the maximum value increases but there is the influence of mainly two frequencies; the fundamental frequency and three times this frequency and there is a very slight influence of the 5th harmonic. This is illustrated in

Figures. 4.5 (e) and (f). An important issue is that at frequencies lower than the resonance frequency the nonlinearity in the velocity is very pronounced; In Figs. 4.5 (b) and (d) can be seen the considerable presence of higher harmonics in the amplitude spectrum of the velocity of the mass at $\Omega = 0.3$ and $\Omega = 0.5$, respectively. The presentence of these higher harmonics with considerable amplitude in the velocity of the mass are due to the high-pass filter effect caused by calculating the velocity from displacement response which possess higher order harmonics as shown in Figs. 4.2 (b) and (d) where the amplitude of the higher order harmonics is small. When the velocity is calculated from such a displacement response, the higher harmonics increases its amplitudes. For instance consider a displacement signal represented in time domain by

$$u(t) = \sin(\omega t) + \frac{1}{2}\sin(3\omega t) + \frac{1}{3}\sin(5\omega t) \tag{4.6}$$

where ω is the an angular frequency and t is time. If $u(t)$ is differentiated in order to obtain velocity it leads to

$$\dot{u}(t) = \omega\cos(\omega t) + \frac{3}{2}\omega\cos(3\omega t) + \frac{5}{3}\omega\cos(5\omega t) \tag{4.7}$$

It can be seen the effect of differentiating a signal composed by several harmonics, it increases the amplitude of the higher harmonics and maintains the amplitude at the fundamental frequency, just as a high-pass filter.

At frequencies higher than the resonance frequency, the velocity amplitude decreases, at $\Omega = 1.5$ the velocity is mainly composed of the fundamental frequency and has a slightly influence of the 3rd harmonic, it is illustrated in Figs. 4.5 (g) and (h). In the isolation region, at $\Omega = 2$, there is just the velocity at the fundamental frequency, evidently because at these frequencies the displacement response is very small (see Figs. 4.5 (i) and (j)).

4.4 Conclusions

In this chapter the reasons why the transmitted force to the base becomes distorted at frequencies close to the resonance region has been investigated. Studying the time history and the spectra of the transmitted force it was found that its high values at the resonance frequency region are produced by the presence of higher harmonics in the transmitted force curves besides the force at the excitation frequency. These high harmonics are markedly presents in the force transmitted through the damper instead of the force transmitted through the spring.

Studying the force through the spring it was found that, specifically for the large amplitude value of the excitation force used here, the maximum force transmitted through it, is close to the amplitude of the excitation force and regardless the excitation frequency it is not larger than the excitation force but at frequencies higher than the resonance frequency the force transmitted through the spring starts to decreases. From the study of the force transmitted through the damper there was found that at frequencies near to the resonance frequency its amplitude exceeds the amplitude of the excitation force.

It was found that for the nonlinear damping force the damping coefficient is amplitude and hence time dependent which is very different compared by a viscous damping coefficient which is constant. It is a nonlinear function whose maximum values are more than one for frequencies below the resonance frequency and less than one for frequencies above the resonance region. That is because the dependence of the nonlinear coefficient on the mass displacement; which at the resonance region is large while at the isolation region is very small.

It was also found that the velocity is the most important cause of the nonlinearity in the damping force because of the presence of high harmonics in its time histories when excited with frequencies corresponding to the resonance frequency region. The presence of high harmonics with considerable amplitudes in the velocity curves is caused by the effect of increasing them when the displacement signal is differentiated which is similar to the effect of a high-pass filter.

It can also be concluded that the nonlinearity of the damping force could be seen as the multiplication of two nonlinearities coming from the nonlinear damping coefficient which increases the amplitude of the harmonics of the velocity of the mass.

5 CONCLUSIONS

5.1 Summary of the Dissertation

This Chapter summarizes the work done in this dissertation and presents the main conclusions obtained as well as the recommendations for further work. The principal goals in this dissertation were to compare the performance between the a linear and a nonlinear vibration isolation system with its damper orientated at ninety degrees with respect to the spring and to analyse the time histories of the transmitted force at frequencies close to the resonance frequency. To achieve these objectives the dissertation was divided as follows:

Chapter 1 introduced the topic of vibration isolation and to present a review of the literature in this area in the specific context of nonlinear vibration isolation.

In Chapter 2 the characteristics of a SDOF linear isolation system when its mass is excited by a harmonic force and when the system is harmonically excited by the base have been reviewed. The equation describing the system in both cases has been obtained to define force and displacement transmissibility for a SDOF isolation system. The way in which the system parameters affect the isolations systems at different frequency regions has been investigated and a discussion about the concepts of transient, steady state and resonance frequency has been presented.

In Chapter 3 the characteristics of a SDOF nonlinear isolation system in which the damper is orientated at ninety degrees to the spring was investigated. Its performance was compared with that of a SDOF isolation system by comparing their force and displacement transmissibilities in the cases in which the systems were excited by a harmonic force and by a harmonic base excitation. A study was undertaken in which low excitation amplitudes were considered. In this case, the nonlinear damping force was approximated to an equivalent viscous damping force. A numerical analysis was conducted for high amplitude excitation.

The force transmissibility for high amplitude excitation levels from Chapter 3 had undesirable performance at frequencies close to the resonance frequency. In

Chapter 4 the time histories for the force transmitted to the base at different frequencies near the resonance frequency and their frequency spectra have been studied. The time histories for the force transmitted through the spring and the force transmitted through the damper together with their spectra have also been studied. Finally, the force transmitted through the damper has been separated into a time dependent damping coefficient and the velocity of the mass to gain some insight into the nonlinear effects.

5.2 Main Conclusions

It has been shown that the force produced by a damper orientated at ninety degrees with respect to the spring can be approximated to an equivalent viscous damping force. It has also been shown that for low amplitude excitation the damping force depends on the square of the relative displacement and it makes the nonlinear isolator suitable for vibration isolation for low levels of excitation.

Analytical expressions have been derived which describe the dynamic behaviour and the performance of the nonlinear isolator for low amplitude excitation. From these it can be concluded that at low amplitude excitation:

- The force and displacement transmissibility at the resonance frequency are smaller than for the linear system provided that $\hat{F}_e \leq \zeta_h / 250$ and $\hat{F}_e \geq 4\sqrt{\left(\zeta^3 / \zeta_h\right)}$ for the force excited system and $\hat{Y} \geq 4\sqrt{\left(\zeta^3 / \zeta_h\right)}$ and $\hat{Y} \leq \zeta_h / 250$ for the base excited system.

- At high frequencies for the force excited system, the nonlinear system performs better than the linear isolator, behaving as if it were undamped. Regarding the displacement transmissibility, the nonlinear system also performs better than the linear system at the resonance frequency but there is a detrimental effect at high frequencies.

For high excitation amplitudes and from the numerical results it has been shown that:

- Regarding the force transmissibility, the nonlinear system at the resonance frequency performs better than the linear system but there is an undesirable effect at frequencies close to the resonance frequency which makes larger the force transmissibility compared with that of the linear system. At high frequencies the nonlinear system performs very well, behaving as if it were undamped. This is one of the important results of this dissertation.

- Regarding the displacement transmissibility close to the resonance frequency, the nonlinear isolator preforms better than the linear isolator but at high frequencies its performance is worse than the linear system.

From the analysis of the time histories and the Fourier series of the transmitted force for the nonlinear system it has been found that the high values close to the resonance frequency are due to the presence of higher harmonics. Decomposing the transmitted force at frequencies close to the resonance region it has been shown that specifically for the large amplitude of the excitation force use in this work; the amplitude of the force transmitted through the spring is not larger than the amplitude of the excitation force. However, this is not the case with the force transmitted through the damper.

Decomposing the force through the nonlinear damper it has been shown that the damping coefficient is not constant but varies with time and is a nonlinear function. It causes an increase in the amplitude of the velocity of the mass at frequencies greater than the resonance frequency and decreases the amplitude of the velocity in the isolation region. It has also been shown that the velocity of the mass is the most important cause of the nonlinear behaviour of the damping force. Finally, it can be concluded that the nonlinearity of the damping force arises from the geometry of the system.

5.3 Recommendation for Further Work

In this work the damper was oriented so that it is at ninety degrees from the spring. Further work can investigate the performance of SDOF isolation systems with different positions of the damper with respect to the spring between 0 and ninety degrees.

Another possibility is to investigate the performance of a SDOF isolation system with two linear springs; one of which is at ninety degrees from the other and is parallel to a linear viscous damper, the external disturbance is applied at ninety degrees to the damper.

The performance of a similar system to that investigated in this work could be studied but considering two degrees of freedom so that the mass can move in the plane formed by the damper axis and the spring axis.

REFERENCES

FULLER, C. R., ELLIOT, S. J., NELSON, P. A. **Active control of vibration**. 1. ed. London: Academic Press Limited, 1996.

HARRIS, C. M., CREDE, C. E.. **Shock and vibration hanbook**. 5. ed. Washington: McGraw Hill Inc, 1961.

LAALEJ, H. et al. Application of non-linear damping to vibration isolation: an experimental study. **Nonlinear Dynamics**, Dordrech, v. 69, n. 69, p. 409-421, 2012.

LANG, Z. Q. et al.Theoretical study of the effects of nonlinear viscous damping on vibration isolation of sdof systems. **Journal of Sound and Vibration**, London, v. 323, n. 1-2, p. 352-365, 2009.

MILOVANOVIC, Z.; KOVACIC, I.; BRENNAN M. J. On the Displacement Transmissibility of a base excited viscously damped nonlinear vibration isolator. **Journal of Vibration and Acoustics**, New York, v. 131, n. 054502, p. 1-7, 2009.

RAO, S. S. **Vibrações mecânicas**. 4. ed. Americana: Pearson Education, 2008.

RAVINDRA, B., MALLIK, A. K. Performance of non-linear vibration isolators under harmonic excitation. **Journal of Sound and Vibration**, London, v. 170, n. 3, p. 325-337, 1994.

RIVIN, E. I. **Passive vibration isolation**. 1. ed. New York: ASME Press, 2003.

RUZICKA J. E.; DERBY, T. F. **Influence of damping in vibration isolation**. 1 ed. Washington: The Shock And Vibration Information Center: Naval Research Laboratory, 1971.

SHIN, K.; HAMMOND, J. K. **Fundamentals of signal processing for sound and vibration engineers**. 1. ed. London: John Wiley & Sons Ltd, 2008.

SNOWDON, J. C. Vibration isolation: use and characterization. **Journal of the Acoustical Society of America**, New York, v. 66, n. 5, p. 1245-1274, 1979.

STEIDEL JÚNIOR, R. F. J. **An Introduction to mechanical vibration**. 3. ed. Washington: John Wiley & Sons, 1989.

TANG, B.; BRENNAN M, J. A Comparison of two nonlinear damping mechanism in a vibration isolator. **Journal of Sound and Vibration**, London, v. 332, n. 3, p. 510-520, 2013.

TANG, B.; BRENNAN; J. M. A comparison of the effects of nonlinear damping on the free vibration of a single-degree-of-freedom system. **Journal of Vibration and Acoustics**, New York, v. 134, n. 024501, p. 1-5, 2012.

THOMSON, W. T., DAHLEH, M. D. **Theory of vibration with application**. 5. ed. New Jersey: Prentice Hall, 1996.

YAN B. **Active vibration isolation with a distributed parameter isolator**. 2007. 250 f. Thesis (PhD in Mechanical Engineering) - University of Southampton, Faculty of Engineering, Science and Mathematics, Institute of Sound and Vibration Research, Southampton, 2007.